INL/EXT-21-64371

Advanced Oxygen Separation from Air Using a Novel Mixed Matrix Membrane

October 2021

Project Final Report

Frederick F. Stewart, Ph.D.
Department Manager, Biological and Chemical Science and Engineering

Idaho National Laboratory

INL is a U.S. Department of Energy National Laboratory operated by Batelle Energy Alliance, LLC

INL/EXT-21-

Advanced Oxygen Separation from Air Using a Novel Mixed Matrix Membrane

Project Final Report

Frederick F. Stewart, Ph.D.
Department Manager
Biological and Chemical Science and Engineering

October 2021

Idaho National Laboratory
Biological and Chemical Science and Engineering
Energy and Environment Science and Technology
Idaho Falls, Idaho 83415

http://www.inl.gov

Prepared for the
U.S. Department of Energy
Office of Fossil Energy
Under DOE Idaho Operations Office
Contract DE-AC07-05ID14517

Page intentionally left blank

FWP Number: # FWP-B000-18-061

Project Title: Advanced Oxygen Separation from Air Using Novel Mixed Matrix Membranes

Principal Investigator:
Frederick F. Stewart, Ph.D.
Manager, Biological and Chemical Science and Engineering Department
Frederick.Stewart@inl.gov
Phone: 208-526-8594

Submission Date: October 2021

Recipient Organization: Idaho National Laboratory, P.O. Box 1625, Idaho Falls, ID 83415
Partner Organization: Argonne National Laboratory, 9700 S. Cass Ave., Argonne, IL 60439

Project/Grant Period: 12/1/2018 – 9/30/2021

Reporting Period End Date: 9/30/2021

Signature of Submitting Official (electronic signatures (i.e., Adobe Acrobat) are acceptable)

Approved by:

October 04, 2021

_____ _____

Frederick F. Stewart Date
Department Manager

Page intentionally left blank

CONTENTS

Page intentionally left blank

ACRONYMS

ARPA-e – Advanced Research Projects Agency - Energy

ANL – Argonne National Laboratory

BP – Budget Period

CAGR – Compound Annual Growth Rate

CNF – Carbon Nanofiber

COOH-ND – Carboxylate-substituted Nanodiamond

CRADA – Cooperative Research and Development Agreement

DOE – Department of Energy

DMAc – N,N-Dimethylacetamide

DMF – N,N-Dimethylformamide

DP – Decision Point

DSC – Differential Scanning Calorimetry

GPU – Gas Permeation Units

HF – Hollow Fiber

INL – Idaho National Laboratory

kWh – Kilowatt Hours

m^2 – Square Meter

MMM – Mixed Matrix Membrane

ND – Nanodiamond

NMP – N-Methylpyrrolidone

PDMS – Polydimethylsiloxane

PI - Polyimide

PPO – Polyphenylene oxide

PVP – Polyvinylpyrrolidone

PSF – Polysulfone

psi – Pounds per Square Inch

PSU – Polysulfone

SEM – Scanning Electron Microscopy

SPP – Strategic Partnership Projects

TEA – Technoeconomic Analysis

T_g – Glass Transition Temperature

TGA – Thermogravimetric Analysis

THF - Tetrahydrofuran

TMA – Thermomechanical Analysis

UTS – Universal Testing System

FIGURES

TABLES

Page intentionally left blank

ABSTRACT

The purpose of this report is to summarize work conducted on project FWP-B000-18-061. In accordance with the Statement of Project Objectives (SOPO), Idaho National Laboratory (INL) in partnership with Argonne National Laboratory (ANL) developed new membrane materials that are well-suited for use in commercially practical oxygen enrichment systems. The technical work was divided into three activities: 1) technoeconomic analysis; 2) membrane component development (support layer, selective layer development, and gutter layer formulation); and 3) hollow fiber formation. The technoeconomic analysis concluded that the desired gas quality (90-95% O_2) cannot be reached with a single stage and that the triple stage system yields the best overall product quality at lower membrane performance levels (O_2/N_2 selectivity of 3.3) but with the highest cost. Using a slightly more selective membrane, selectivity of 5.5, allows for a two-stage system with the lowest cost. For the membrane development activities, functionalized nanodiamonds were shown to slightly improve membrane formation behaviors and gas permeability performance. For example, fabricated support layers based on polysulfone-nanodiamond composites showed an increase in the material's O_2 permeability by over a factor of 150, however, at the cost of selectivity consistent with increased porosity. Furthermore, nanodiamonds were found to improve membrane durability and improvements in selective and gutter layers were also accomplished. Advances in the hollow fiber formation studies resulted in the demonstration of phase inversion of polysulfone-nanodiamond composites, which ensures that hollow fiber formation can be performed. Finally, the interactions between support, gutter, and selective layers were briefly examined and the resulting multilayer membranes showed good air separation performance. The un-optimized three-layer prototype membrane gave permeability of 29.2-32.2 Barrers, which equates to permeance of approximately 290-320 GPU, lower than the TEA informed goal of 500 GPU. O_2/N_2 selectivity ranged from 5.2-6.2, which is consistent with the less costly two-stage implementation of the technology. In summary, new materials have been developed for air separation that are well-suited to a hollow fiber format.

Page intentionally left blank

1. ACCOMPLISHMENTS:

1.1 What are the major goals of the project?

The main objective of this project is to improve upon the state of the art in membrane performance to enable a viable and less energy intensive alternative to cryogenics, pressure swing absorption, or high temperature ionic membrane processes for separating O_2 from air to yield a 90-95% O_2 stream that is specifically designed to support small modular coal fired power or gasification plants.

The technical thrust of this work is to avoid the pitfalls associated with membrane scale-up and commercialization by improving upon existing engineering. Thus, the experiments performed in this project are directed towards modifying mature technology with novel approaches so that the membrane attributes that make them suitable for manufacturing are not lost. This approach holds the promise of improved membrane performance and durability while de-risking deployment of technology.

Idaho National Laboratory's (INL's) and Argonne National Laboratory's (ANL's) pathway to meet this goal is the development of a mixed matrix membrane (MMM) that will consist of a predictable and well-characterized polymer host and a novel particle/facilitator based upon nanodiamond (ND) technology. NDs are sp^3 hybridized carbon nanoparticles that are commercially available and have largely been unexplored for their ability to facilitate selective gas transport in polymer materials.

To support the objective, there are several aspects that must be considered. First, a baseline of performance must be established. This will consist of permeability/selectivity measurements on pure polysulfone (PSF), polyphenylene oxide (PPO), and polydimethylsiloxane (PDMS) membranes. PSF is being considered for the hollow fiber support, PPO for the selective layer, and PDMS as a gutter layer. Second, the range of available ND characteristics must be included into the decision-making process. The permeability of a membrane is the product of its diffusivity for a specific gas and the solubility of that gas within the polymer. NDs are expected to influence both diffusivity and solubility of the gases within the membrane. Selection of the correct characteristics is considered critical to the success of the project. Third, membrane formation behaviors are important. The introduction of NDs cannot disrupt or otherwise prevent the facile formation of either thin dense film or hollow fiber (HF) membranes.

Critical barriers and challenges that were addressed in the work scope are:

- Poor permeance and selectivity of polymeric membranes
- Conversion from flat sheet to hollow fiber formats – phase inversion to introduce support porosity.
- The need for improved performance of individual proposed hollow fiber layers
- Balance the need for minimal layer thickness with defect structures.

This report is a summary of Budget Period (BP) 1 and 2 activities. Specific tasks that support the technical objectives of this work in overcoming the barriers and challenges are:

Task 1. Project Management and Planning. This was an on-going task that spanned the lifetime of the project. This task resources all required reporting and project management. Also, under this task, steady regular communication with ANL was maintained with the purpose of sharing data and ideas for further membrane development.

Task 2. Membrane Development. This task was divided into three subtasks that correspond to the functional layers of the proposed hollow fiber membrane: 1) support; 2) selective; and 3) gutter. Figure 1 is a graphic abstract of the development effort with critical aspects identified.

Task 3. Membrane Characterization. This task provided the data on membrane structure and performance. This task was tied to Tasks 2, 4, and 5. In support of Task 2, permeability, selectivity, and microscopy measurements are shown in this task.

Task 4. HF Fabrication Development. The goal of this task was to ensure that modified PSF materials will undergo phase inversion. As described in Task 2, with the success of the initial phase inversion experiments conducted on PSF-ND MMMs, we greatly de-risked the formation of hollow fiber membranes.

Task 5. Module Development. This was a BP3 planned activity – no work on performed on this task. Tasks include formation of a hollow fiber bundle that potted using standard techniques into a suitable tubular housing with machined ports to allow for gas flow down the inner channels of the hollow fibers and for permeated gas to be collected in the outer shell. This task was to use hollow fiber designs developed in Task 4.

Task 6. Modeling/TEA. This task was completed and produced: 1) targets for membrane performance and one peer-reviewed publication.

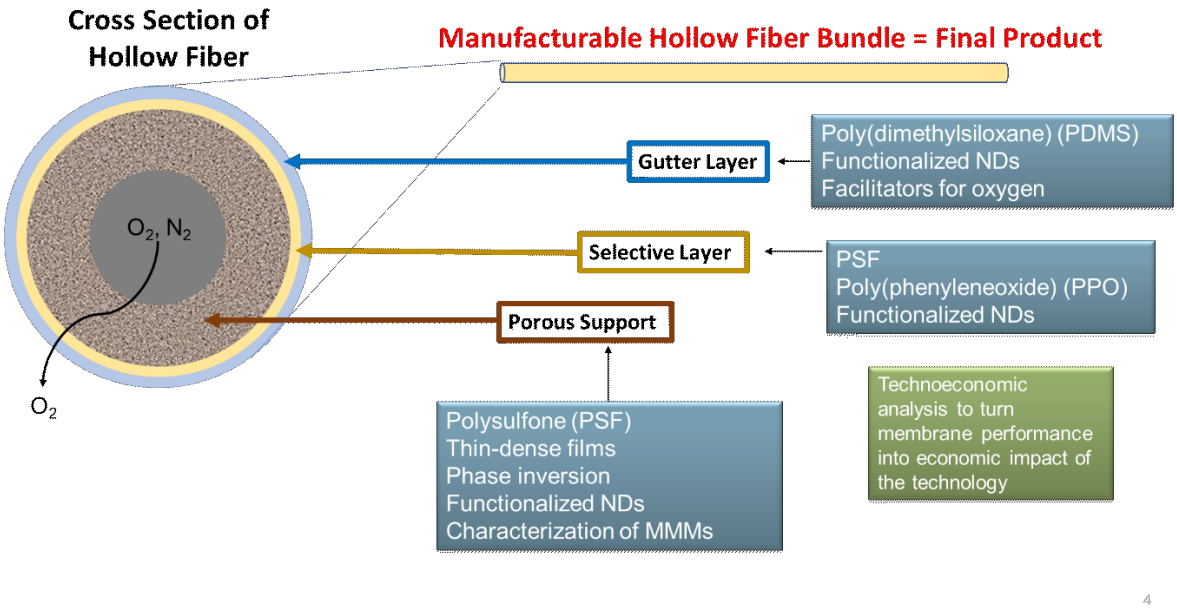

Figure 1. Graphical abstract of the project activities.

Table 1. Project Milestone Status Update.

Milestone Number and Task	Milestone Title	Planned Completion Date	Actual Completion Date	Variance Comment	Verification Method (if complete; e.g., summary report, quarterly progress report)
BP1, M1, Task 1	Updated Project Management Plan	1/01/19	10/16/18		Email
BP1, M2, Task 1	Kickoff Meeting	2/01/19	1/22/19		Webinar

Milestone Number and Task	Milestone Title	Planned Completion Date	Actual Completion Date	Variance Comment	Verification Method (if complete; e.g., summary report, quarterly progress report)
BP1, M3, Task 1	Inter-lab transfer of funds to ANL	3/01/19	2/15/19		Email
BP1, M4, Task 3	Complete study of flat sheet membranes suitable for publication	11/30/19	11/30/19		Quarterly Report
BP1, M5, Task 3	Complete initial flat sheet membrane formation study to demonstrate defect-free films can be made, optimize ND loading	10/30/19	10/15/19		BP1 Final report
BP2, M6, Task 3 (formulation. data from Task 2 and the characterization data is derived in Task 3)	Completion of a comparative study of polysulfone with and without NDs. Permeability and selectivity of membrane using O_2, N_2, and other select gases to understand the effect of ND inclusion in the polymer materials	5/31/2020	9/30/2021		Data including synthesis and characterization has been collected.
BP2, DP1, Task 4	Go/no-go decision point for development of ND composite HF	11/30/20	9/30/21	Delayed by funding lapse (February 2020) and COVID-19 (March-June). Decision point was judged to be a "no go" based on changed program priorities. A no-cost extension of the project was granted to 9/30/2021.	Performance data, excel spreadsheet. O2/N2 selectivity greater than or equal to 3.3 – 5.5 as recommended by the TEA.

Milestone Number and Task	Milestone Title	Planned Completion Date	Actual Completion Date	Variance Comment	Verification Method (if complete; e.g., summary report, quarterly progress report)
BP2, R3	Shift the research priority from flat sheet testing and development to hollow fiber membrane development and testing based on the flat sheet data that has already been generated, especially for gutter and selective membrane materials.	9/30/21	9/30/21		Project Final Report and Close-out Presentation
BP2, R4	Produce and test multilayer membranes to examine possible delamination or layer interaction effects on performance and impacts on permeation properties.	9/30/21	9/30/21		Project Final Report and Close-out Presentation
BP2, R6	Provide the O2 recovery and energy consumed per mole of O2 produced metrics (e.g., $/ton O2, O2 purity, O2 recovery, energy consumed/mole of O2 produced, stage cut, moles of O2 produced per square meter of membrane area) in a report to DOE.	9/30/21	9/30/21		Project Final Report and Close-out Presentation

1.2 What was accomplished under these goals?

1.2.1 Task 1. Project Management and Planning. All tasks associated with project management are completed.

1.2.2 Task 2. Membrane Development. This task has been divided into three subtasks that correspond to the functional layers of the proposed hollow fiber membrane: 1) support; 2) selective; and 3) gutter.

1.2.2.1 Subtask 2.1. Support layer development. A sampling of gas permeation literature data for polysulfone (PSF) mixed matrix membrane (MMM) materials is shown in Table 2. In general, some influence on the membrane performance is seen through the inclusion of additives where permeability can be increased but at the cost of selectivity.

Data generated at ANL characterized pure PSF as a function of temperature, Table 3 and Figure 2. Permeability data for O_2 largely agreed with previous data taken at INL. Increasing the temperature at which the membrane is operated results in expected increases in permeability.

Nanodiamonds. Nanodiamonds have been acquired and incorporated into PSF polymers (PSF-ND) forming MMMs. NDs have been procured with several differing types of functionality, as shown in Table 4. NDs are of interest because it was believed that they can influence both the diffusivity and solubility of O_2 in and through a PSF membrane.

NDs can be formed either as individual nanoparticles with an approximate diameter of 5 nm, or as clusters up to 500 nm in size. It is thought that the clustering can bring intrinsic porosity into the MMMs resulting in a potentially controllable method to encourage O_2 selectivity.

Surface functionalization has been developed in NDs to influence surface charge characteristics so that they can be dispersed into liquids ranging from non-polar motor oil to polar tetrahydrofuran (THF). Using this methodology, it was envisioned that through adroit choice of surface functionality, increased solubility of O_2 within the membrane could be possible. An example is the attachment of long chain alkyl groups, where these chains can exhibit some gas solubility and may plasticize the polymer host locally around the ND, thus encouraging permeability.

Table 2. Benchmark data for PSF MMM materials.

Membrane Material	O_2 Permeability (Barrers)	O_2/N_2 Selectivity	Additive	Reference
Project Goal	10 (100 GPU)	6	Functionalized Nanodiamond	-
PSF/CNF mixed matrix	2.2	3.86	Carbon Nanofiber	[1]
PSF with 20 % silica nanoparticles	5.0	4.50	Silica	[2]
PSF with 5 % CX Fiber	1.78	5.95	Pyrolytic Carbon Xerogel (PDMS gutter layer)	[3]
PSF with 5 % CX Fiber	17.5	1.13	Pyrolytic Carbon Xerogel (no gutter layer)	[3]
Pure PSF	1.2	6	None	[4]

Table 3. Initial PSF data taken at ANL.

Temp, °C	O_2 (Barrer)	N_2 (Barrer)	Ideal selectivity (O_2/N_2)
24	1.3	0.3*	3.8
55	2.4	0.4*	6.1
99	4.6	1.1	4.3

*not reliable due to very low nitrogen flux (≈$7*10^{-5}$ ml/min-cm^2)

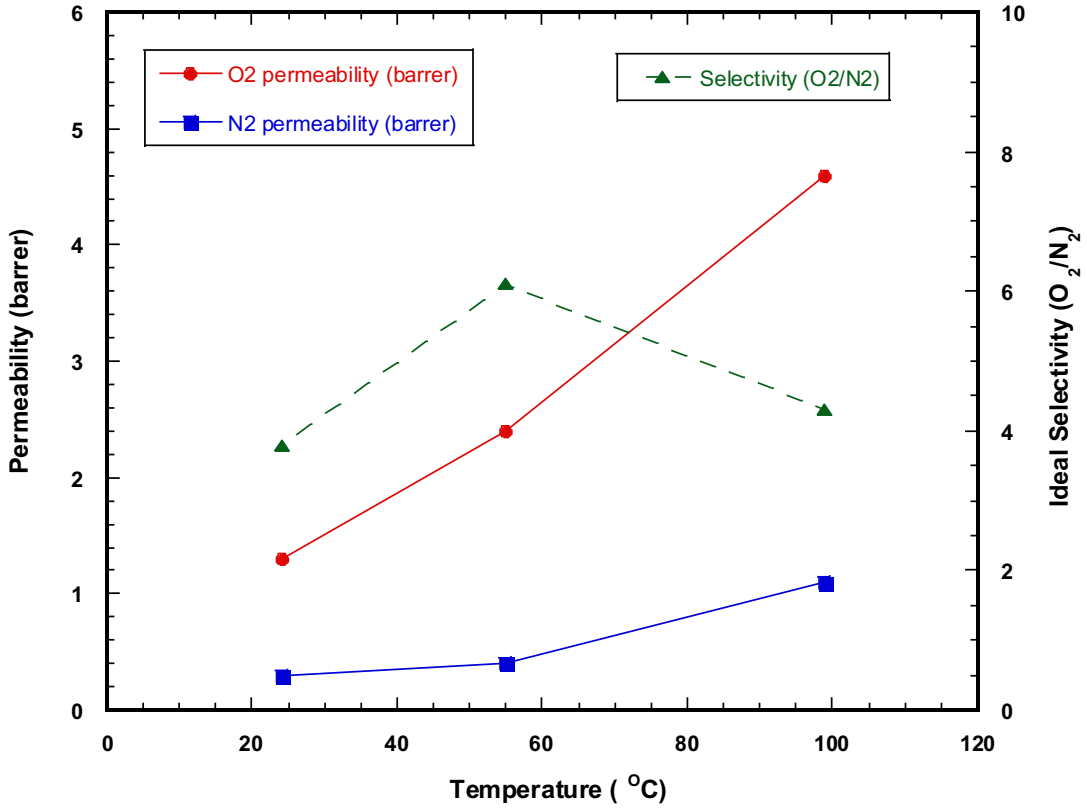

Figure 2. Plot of O_2 and N_2 permeability through PSF as a function of temperature.

Table 4. NDs of interest in this work.

Nanodiamond surface functionality	Characteristics
Carboxylic acid/carboxylate (COOH)	Negative zeta potential useful for suspending in solvent. Native state of the ND after separation from carbon black.
Alkyl chains (C_6, C_{12}, and C_{18})	Non-polar, potentially valuable for dispersion in both solvent and polymer hosts.
Perfluoro-group (-CF_2H)	Prepared by plasma substitution in CF_2H_2 gas. Non-polar. Potential for O_2 affinity.
Perfluoro-group (-$OCH_2CF_2CF_2H$)	Prepared through wet chemical functionalization. Non-polar. Potential for O_2 affinity.

PSF MMMs with COOH functionalized NDs. A literature review of ND containing MMMs for use as gas separating membranes yielded only 3 papers, all from the same group, Table 5. In the first paper, a polyimide-ND MMM was formed with 1 % loading of carboxylic acid functionalized ND (COOH-ND). The O_2/N_2 gas pair was not reported, but an analysis of the H_2/CO_2 gas pair revealed that the permeability of the more permeable gas, H_2, was slightly reduced upon the addition of NDs.

Table 5. Literature data for ND containing MMMs.

Membrane Polymer	Permeability (Barrer)	Selectivity	Additive	Reference
Project Goal	O_2 = 10	O_2/N_2 = 6	Functionalized Nanodiamond	-
P84 co-polyimide	H_2 = 8.0	H_2/CO_2 = 3.6	None	[5]
	H_2 = 6.7	H2/CO_2 = 4.1	1 % ND (COOH)	
Poly(phenyleneoxide) (PPO)	O_2 = 33.2	O_2/N_2 = 3.25	None	[6]
	31.8	3.61	1 % ND (COOH)	
	29.7	3.81	3 % ND (COOH)	
	28.4	4.06	5 % ND (COOH)	
Poly(phenylene-isophthalamide)	O_2 = 0.032	O_2/N_2 = 5.9	None	[7]
	0.029	6.3	1 % ND (COOH)	
	0.029	10.0	3 % ND (COOH)	
	0.017	1.2	5 % ND (COOH)	

A second paper discusses the inclusion of COOH-NDs into PPO at loadings of 1 %, 3 %, and 5 %. O_2 permeability of native PPO was a relatively high at 33.2 Barrers. Addition of COOH-NDs resulted in slight loss of permeability (down to 28.4 Barrers at 5 % loading) as a function of loading with a concurrent

increase in selectivity (increasing from 3.25 to 4.06 at 5 % loading). The high permeability and compatibility of the polymer with NDs is interesting and was of value to this project.

Table 6. PSF/ND-COOH mixed matrix membranes.

Membrane composition (UDEL PSF Cast from NMP)	O_2 Permeability (Barrers)	O_2/N_2 Selectivity	Notes
No NDs	0.73	6.1	
2 % 5nm-COOH ND	0.72	6.5	With increased selectivity, chosen for a temperature study
5 % 5 nm-COOH ND	0.41	2.6	Defects?
10 % 5 nm-COOH ND	NA	NA	Membrane shattered, testing not possible

In the third paper, membranes were formed from poly(phenylene-isophthalamide) at loadings of 1 %, 3 %, and 5 % COOH-ND. Very low O_2 permeabilities are reported; however, the same trend of loss of permeability with an increased loading of COOH-ND was observed.

In our laboratories, 5 nm COOH functionalized ND particles were acquired as suspensions in solvent. For the initial work, n-methylpyrrolidone (NMP) solvent was selected for two reasons: 1) it solvates both PSF and NDs well and 2) it is commercially used in the formation of hollow fiber membranes due to its low volatility and safety. PSF membranes were formed with 2 %, 5 %, and 10 % COOH-ND and data for O_2 permeability and O_2/N_2 selectivity are shown in Table 6. Without added NDs, the "as cast" PSF membranes gave a permeability of 0.73 Barrers with an O_2/N_2 selectivity of 6.1. Addition of COOH-ND at 2 % resulted in a slight loss of permeability and an increase in selectivity, consistent with the literature reports. Increasing the loading to 5 % resulted in a loss of both permeability and selectivity, which was not expected. The reduction in permeability and selectivity with higher loading values may be attributed to the formation of structure defects, supporting this was the experiment conducted using a 10 % ND loading, which resulted in membranes with insufficient mechanical integrity to be tested for gas permeability.

Table 7. MMMs formed with COOH-ND clusters.

Membrane composition (UDEL PSF Cast from NMP)	O_2 Permeability (Barrers)	O_2/N_2 Selectivity	Notes
2 % 30-50 nm-COOH ND	0.74	4.5	100 ^{O}C for 1 Hour
10 % 30-50 nm-COOH ND	0.62	4	100 ^{O}C for 1 Hour
2 % 30-50 nm-COOH ND	0.19	6.4	100 ^{O}C for 1 Hour, 75 ^{O}C under vacuum for 72 hrs

To probe whether ND clustering, which should create porosity through the clusters, can contribute to permeability, a study using 2 % and 10 % loadings of 30-50 nm clusters of COOH-NDs was initiated, Table 7. Membranes with 2 % and 10 % loadings were prepared with drying at 100 °C. Permeability studies of the membranes produced the same trend as seen for the individual particles, decreasing O_2 permeability with increasing ND loading. However, one additional factor was observed – the selectivities were less than expected. To understand if the drying conditions played a role in lowering selectivity, a second drying step in a vacuum oven at 75 °C was used. Data for this membrane saw significant loss in permeability, but an increase in selectivity to > 6. This work suggested that the thermal treatment impacted membrane performance, and this could be due to aging (material densification) or loss of remaining solvent.

The importance of solvent removal. Much work was done to effectively form membranes and understand their permeability behavior with respect to varying conditions. The experiments showed that the removal of solvent was a paramount concern.

Thermogravimetric Analysis (TGA) was employed to probe the membranes for residual solvent. NMP is a high boiling solvent at 202 °C. Rigorous drying was shown to yield a membrane that consisted of 20 % residual solvent, Figure 3. In this plot, solvent loss was still occurring at temperatures as high as 400 °C. To reduce the solvent content, the membrane was soaked for 26 hours in water to leach out water miscible NMP. This reduced the solvent content by about 75 %, Figure 4; however significant solvent remained, which would be expected to influence membrane transport. As a final determination that the mass loss in these experiments was due to residual NMP, the solvent was replaced with tetrahydrofuran that has a boiling point of 66 °C. Another aspect in the solvent selection is that membrane materials can anneal and densify with heat treatment, which has the potential to lower permeability. Thus, it is best to use solvents that do not require aggressive heat treatments, such as THF.

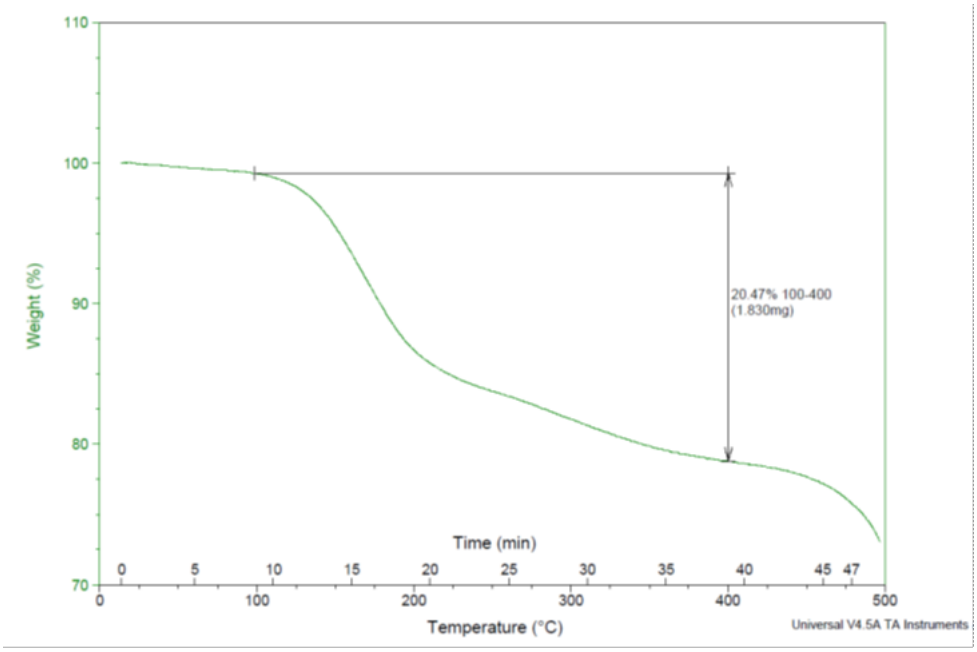

Figure 3. TGA temperature ramp for PSF cast from NMP.

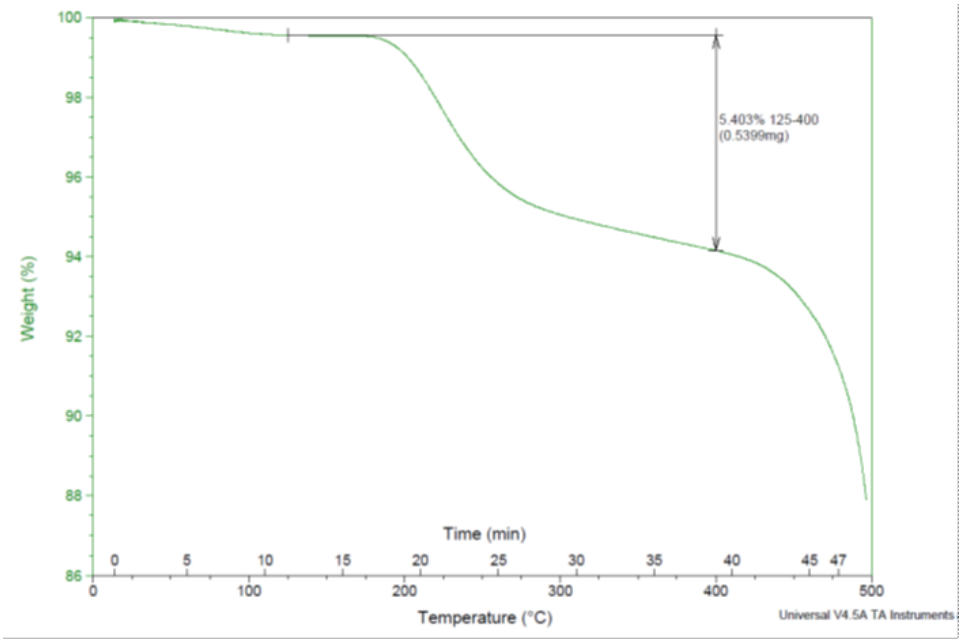

Figure 4. TGA analysis of PSF soaked in water for 26 hours.

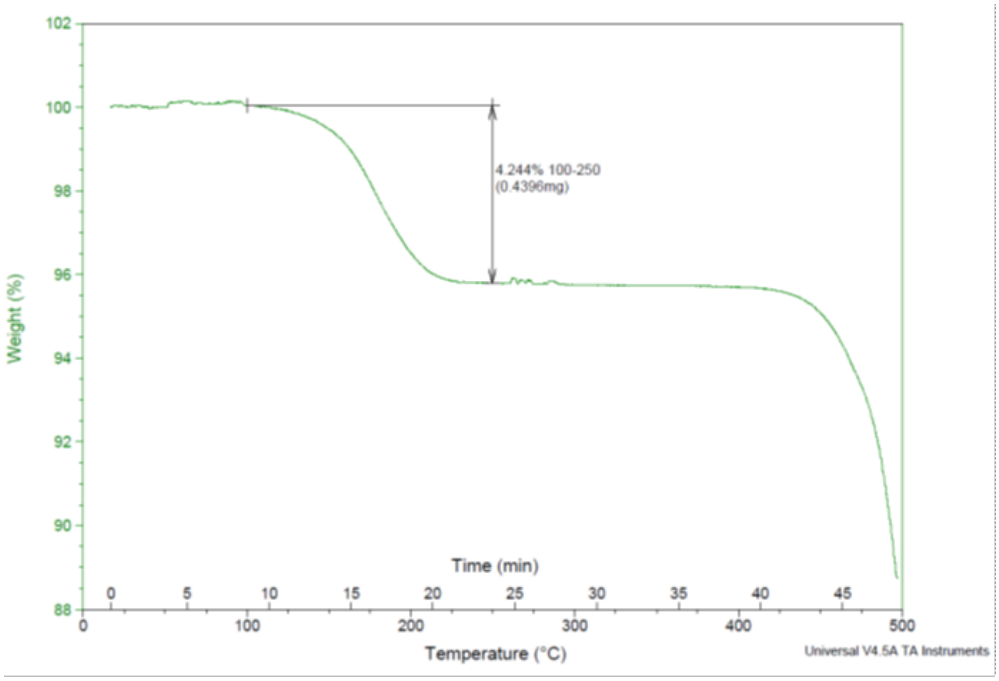

Figure 5. TGA analysis of PSF cast from THF.

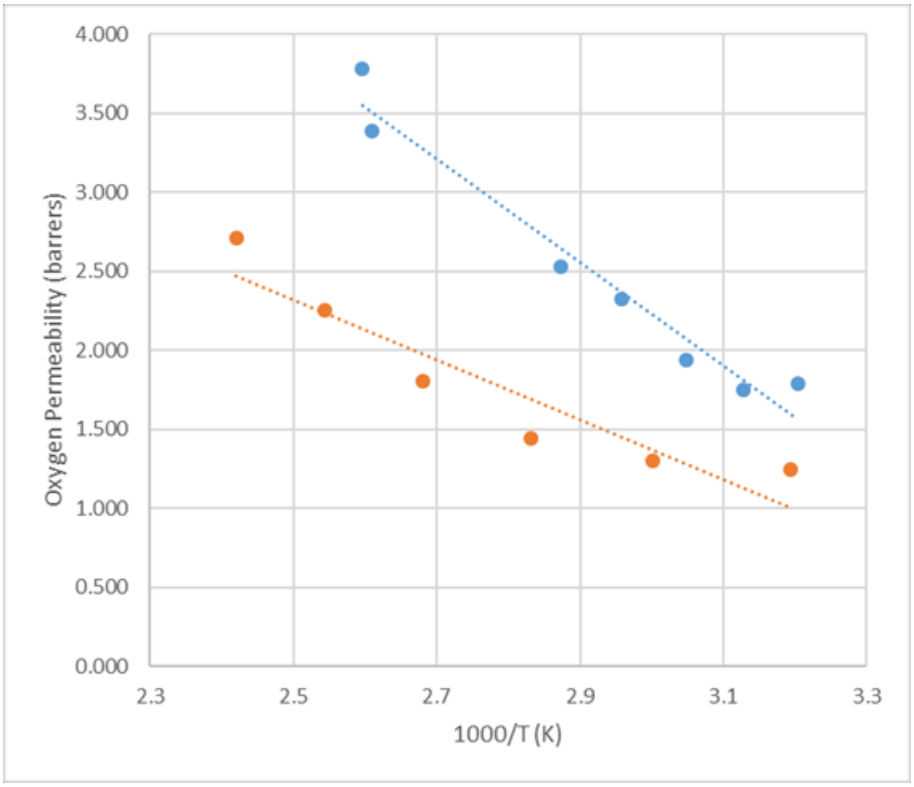

Figure 6. O_2 permeability of PSF membrane (orange data) and PSF with 2 % COOH-ND loading (blue data).

THF is not an ideal solvent for hollow fiber formation due to its volatility, flammability and toxicity. However, it is a good solvent for diagnostic purposes because of its low boiling point. Membranes prepared using THF as the solvent were prepared similarly to the NMP. TGA of PSF cast from THF, given in Figure 5, shows the loss of residual solvent. Significantly, solvent loss is seen up to 200 °C, which is well above the boiling point for THF; this suggests that there is physical solvent entrainment in the polymer. Furthermore, it is not clear what role NDs play in this solvent entrainment. Use of TGA combined with mass spectrometry detection revealed that a portion of the mass loss was water, which was most likely a THF contaminant.

Rigorous removal of THF was accomplished on thin dense film membranes by raising the temperature to 200 °C. Gas permeation testing of membranes with 2 % loading of COOH-NDs were prepared. O_2 permeability was found to increase with this loading of NDs, contrary to the earlier work in both the literature and in our labs. A study of O_2 permeability as a function of temperature is shown in Figure 6. *This work suggested that solvent removal was critical to the development of higher performing PSF-ND composite MMMs.*

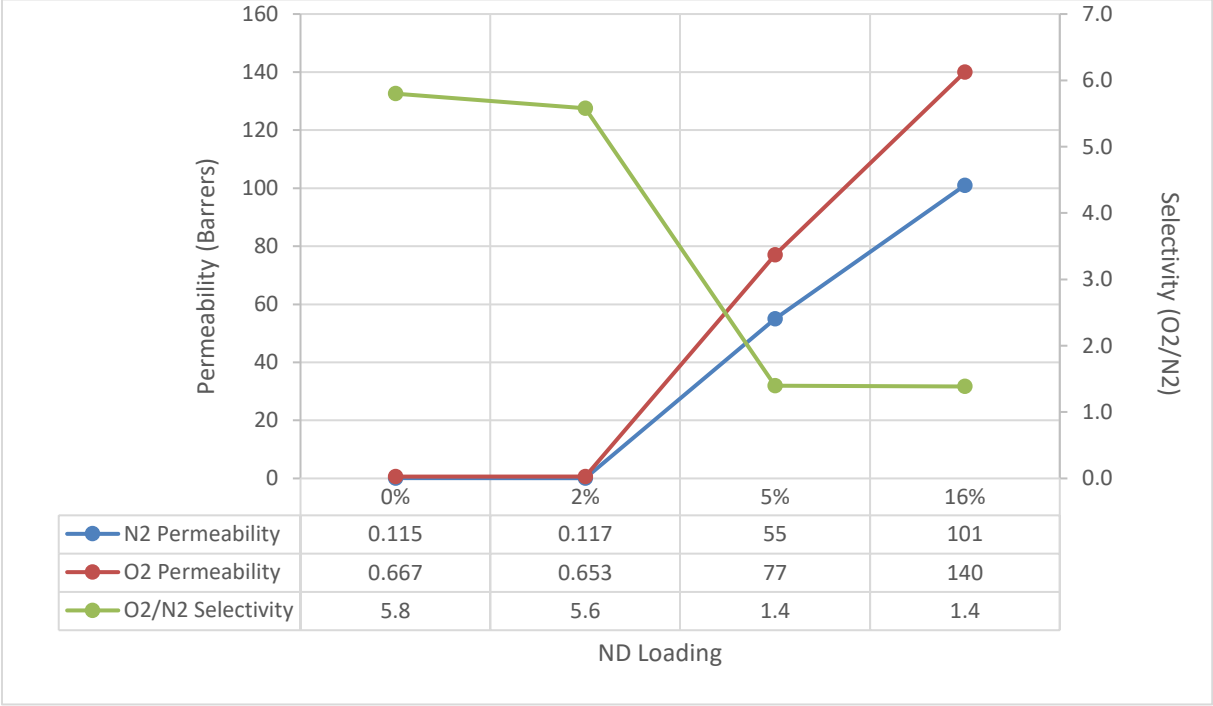

Figure 7. O_2 (blue data) and N_2 (orange data) permeability and selectivity (gray data) of PSF membranes with loaded with 2 %, 5 % and 16 % C18-NDs.

PSF MMMs with C_{18} functionalized NDs. C_{18}-NDs have linear aliphatic (C_{18}) chains attached to the surface of the nanodiamond particle. These groups serve to alter the chemical and physical characteristics of the particle and are of interest to this project because 1) it was thought that they could further disrupt polymer chain stacking due to their increased size, and 2) they might provide an alternate pathway for gas permeation. Figure 7 shows O_2 and N_2 permeability data for membranes with loadings of C_{18}-NDs at 2 %, 5 %, and 16 %. Immediately, it can be seen that much higher loading of C_{18}-NDs could be achieved when compared to the COOH-NDs, where 10 % resulted in membrane fragmentation. It is possible that the long alkyl chains will penetrate into the polymer chains and stabilize the physical characteristics of the membrane. Strengthening of polymers with COOH-NDs has been reported in the literature [10] and this result suggests that C_{18} functionalized NDs may be more effective than COOH-NDs at imparting durability.

Further examination of the permeability data in Figure 7 reveals some other startling results. At 2 %, no real change was seen with data nearly identical to that of pristine PSF (0 %). However, at 5 %, P_{O2} was observed to increase 120-fold, with a similar significant increase in N_2 permeability as well, suggesting a change in transport mechanism. Selectivity drastically decreased to ~1.4, however, the fact that the material is somewhat O_2 selective suggests that the transport is not entirely due to defect structure formation.

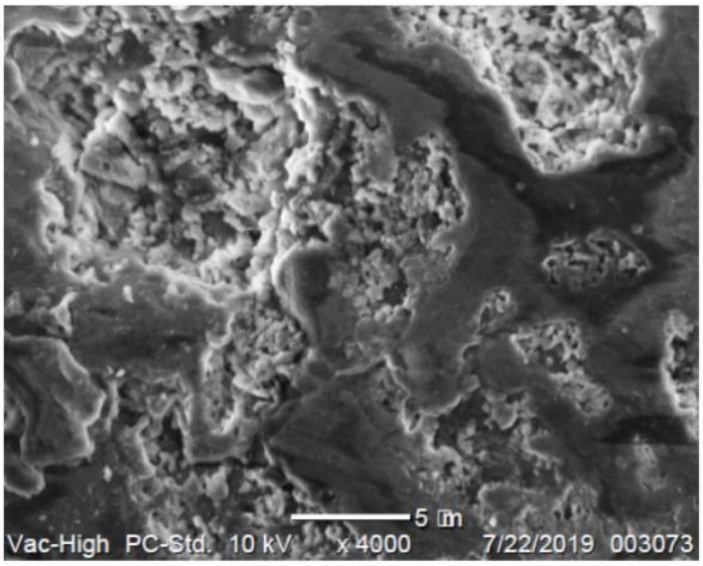

Figure 8. SEM image of PSF with 16 % C_{18} ND loading.

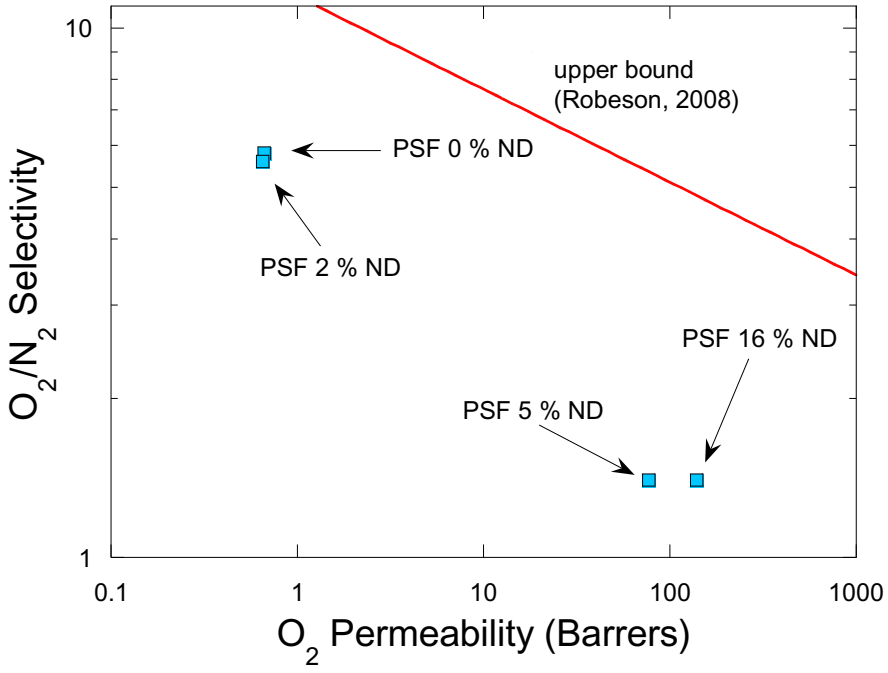

Figure 9. Permeability/selectivity plot for PSF with 0 %, 1 %, 5 %, and 16 % ND loading.

Increasing the loading to 16 % resulted in permeability of both gases increasing by a factor of 2, with respect to the 5 % membrane; whereas, the selectivity did not change and remained at O_2/N_2 = 1.4. An initial analysis of the morphology of these materials was performed by scanning electron microscopy (SEM), Figure 8. Regions of microporosity in the 16 % C_{18}-ND loaded PSF are clearly visible as well as regions of homogenous PSF.

Plotting this data on a permeability versus selectivity plot (Figure 9) reveals the change in performance with respect to a theoretic upper bound. This analysis is a commonly applied approach to visualize the trade-off in membrane performance between permeability and selectivity. [8] The data clearly is bimodal between the 0 % and 2 % materials and the 5 % and 16 % ND loaded membranes. The performance moves roughly parallel to the upper bound, which suggests that the increase in permeability at higher ND loadings is offset by lower selectivity. A goal of this project is to develop materials that can approach the upper bound.

1.2.2.2 Subtask 2.2. Selective layer development. The goal of the selective layer is to provide the selectivity of O_2 over N_2 with as small an impact on the overall permeability as possible. For hollow fiber construction, the selective layer can be a dense layer of polymer formed during phase inversion or a coating placed on the fiber after formation. Although PSF forms durable membranes, the permeability of the polymer is not as high as it needs to be. Thus, an alternate polymer material whose base performance offers higher permeability while retaining selectivity near 6 was chosen.

Poly(phenylene oxide) (PPO) is an interesting material since it could be an effective coating with improved physical durability. Table 8 is a comparison of literature data for PPO (also shown in Table 5) that shows P_{O2} of 33.2 Barrers without NDs, which slightly decreases with increasing COOH-ND loading. As compared to literature PSF performance, PPO clearly offers about a 28-fold improvement in permeability with a slightly lower selectivity of 3.25. It was envisioned that selectivity could be raised, which will result in lower P_{O2}.

Table 8. Selected literature and experimental data for the selective layer.

Membrane Polymer	O_2 Permeability (Barrer)	O_2/N_2 Selectivity	Additive	Notes
PPO	33.2	3.25	None	[6]
	31.8	3.61	1 % ND (COOH)	
	29.7	3.81	3 % ND (COOH)	
	28.4	4.06	5 % ND (COOH)	
PPO	33.4	3.4	None	Cast from Toluene at INL, Dried at 75 °C, 72 hrs
PPO	7.4	4.6	2 % C18 NDs	Cast from DMAc
PPO	28.8	4.4	2 % C18 NDs	Cast from Toluene at INL, Dried at 75 °C, 72 hrs

Reproduction of literature data was achieved for PPO with a permeability of 33.4 Barrers, which corresponds to 330 GPU and a selectivity of 3.4. Addition of C18-NDs in N,N-dimethylacetamide (DMAc) solvent to PPO resulted in lower P_{O2} of 7.4 Barrers, but with improved selectivity of 4.6. Changing the casting solvent to toluene, which has a significantly lower boiling point of 110 °C and drying the membrane at 75 °C in a vacuum oven prior to analysis shows improved P_{O2} of 28.8 Barrers with a selectivity of 4.4.

This solvent effect is consistent with the support layer PSF data that suggests that solvent can negatively impact membrane performance and that it is critical to remove solvents completely.

For this technology to be successful, the selective layer, which represents the least permeable part of the multilayer format, must give an O_2 permeability of 35-50 Barrers. A surfactant was used to modify the chemical affinity of the NDs, leading to enhanced selective layer performance due to improved interactions between the particle and host. [11] Furthermore, the particle surface modifier ensures the particle has the ability to be suspended in common solvents and ensures maximum particle distribution within the polymer host. Table 9 shows the gas permeability data for cast and heat processed PPO without NDs, and with 1 % and 2 % loadings. Without NDs, PPO cast from toluene and dried at 75 °C gives an oxygen permeability (P_{O2}) of 33.4 Barrers and a nitrogen permeability (P_{N2}) of 9.8, which gives an O_2/N_2 selectivity of 3.4.

Table 9. Permeability and selectivity data for selected PPO/ND composites.

Membrane	**P_{O2} (Barrers)**	**P_{N2} (Barrers)**	**O_2/N_2**
Pristine PPO cast from toluene, processed at 75 °C	33.4	9.8	3.4
PPO with 1 % NDs cast from toluene and processed at 100 °C	11.6	2.4	4.8
PPO with 2 % NDs cast from toluene and processed at 100 °C	9.5	2.5	3.8
PPO with 2 % NDs cast from toluene and processed at 150 °C	37.6	11.2	3.7

At 1 % and 2 % ND loadings processed at 100 °C clearly showed declining performance where P_{O2} values dropped substantially. However, the increase in selectivity of the 1 % composite is intriguing. To probe the cause of the permeability decline, the 2 % experiment was repeated but the membrane was processed at higher temperature, which caused P_{O2} to increase to levels seen for the unmodified polymer. This experiment suggests that solvent inclusion can block permeation channels within the membrane, thus depressing permeability. This was seen in the permeability data for both gases.

Additional work was conducted to minimize the thickness of the PPO layer. PPO is not an easy polymer to form consistent thickness defect-free films. Several solvents were explored in this work including NMP, DMAc, toluene, and THF, for their use as an effective casting solvent that is compatible with the other components of the membrane. Xylene was found to yield good films with thicknesses ranging from 2-5 µm. This knowledge can be directly applied to a proposed hollow fiber coating procedure.

1.2.2.3 Subtask 2.3. Gutter layer development.

Neat PDMS. Poly(dimethylsiloxane) (PDMS) is commonly used as a gutter layer due to its low cost, excellent coating properties, relatively high gas permeability, and easy application process. The purpose of the gutter layer is to patch defects in the support layer that cannot be bridged by the selective layer. Analysis of newly cast PDMS membranes was accomplished using a 40%/60% O_2/N_2 feed gas mixture at

temperatures ranging from 24 to 125 °C, Figure 10. The expected trend of increasing permeability and decreasing selectivity with increased temperature was observed.

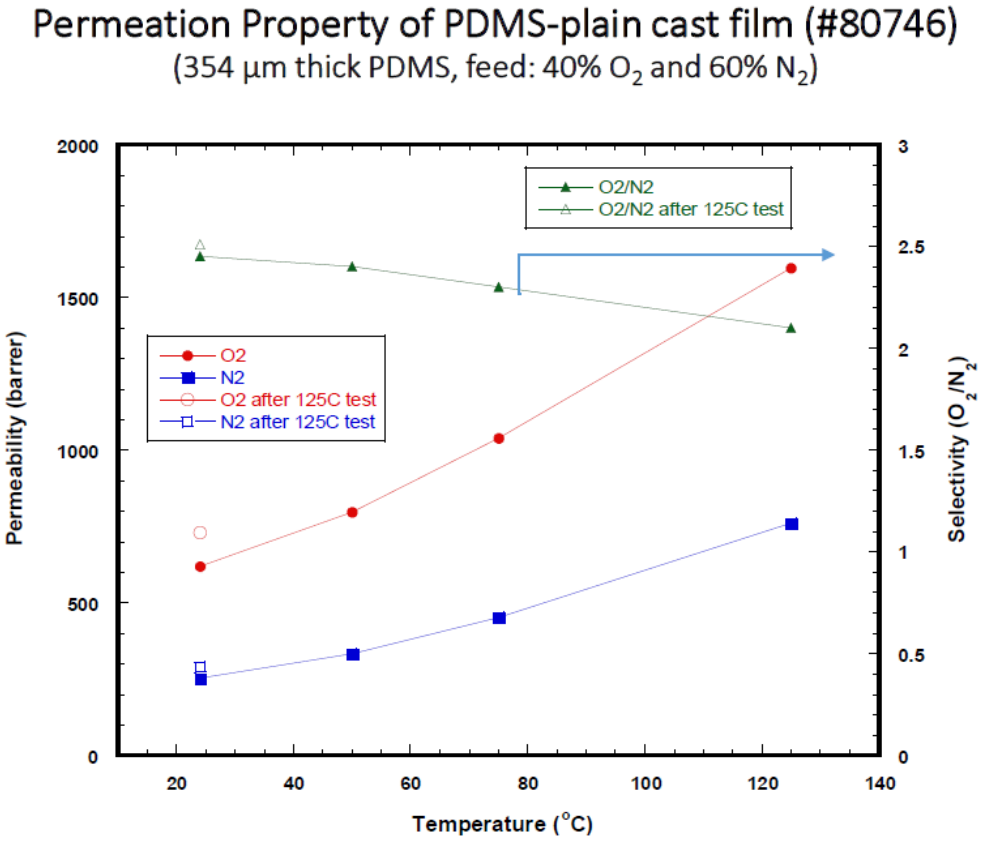

Figure 10. Variable temperature performance of PDMS against O_2/N_2.

Since membrane performance can vary as a function of feed gas composition, PDMS was analyzed over three differing compositions: 40%/60% O_2/N_2, 60%/40% O_2/N_2, and 20 % each of O_2 and N_2, with the balance Helium. Figure 11 shows that the P_{O2} and P_{N2} values are consistent across the gas composition profiles with some deviations in the lower temperature selectivity which was largely due to some deviations in the P_{N2} measurement.

Additives. To produce improved gutter layers with more selectivity and increased P_{O2}, studies were undertaken to use both NDs and cobalt containing inorganic facilitators to improve performance of PDMS. The NDs chosen for this work are the C_{18} functionalized and were chosen because it was thought that the long alkyl chains would encourage compatibility with PDMS. As shown in Figure 12, there was an approximate 20 % increase in P_{O2} with the addition of NDs or the facilitator. However, neither the addition of the facilitator nor NDs appear to decrease the selectivity of PDMS, not justifying the cost of using additives and leading to an end in this area of research.

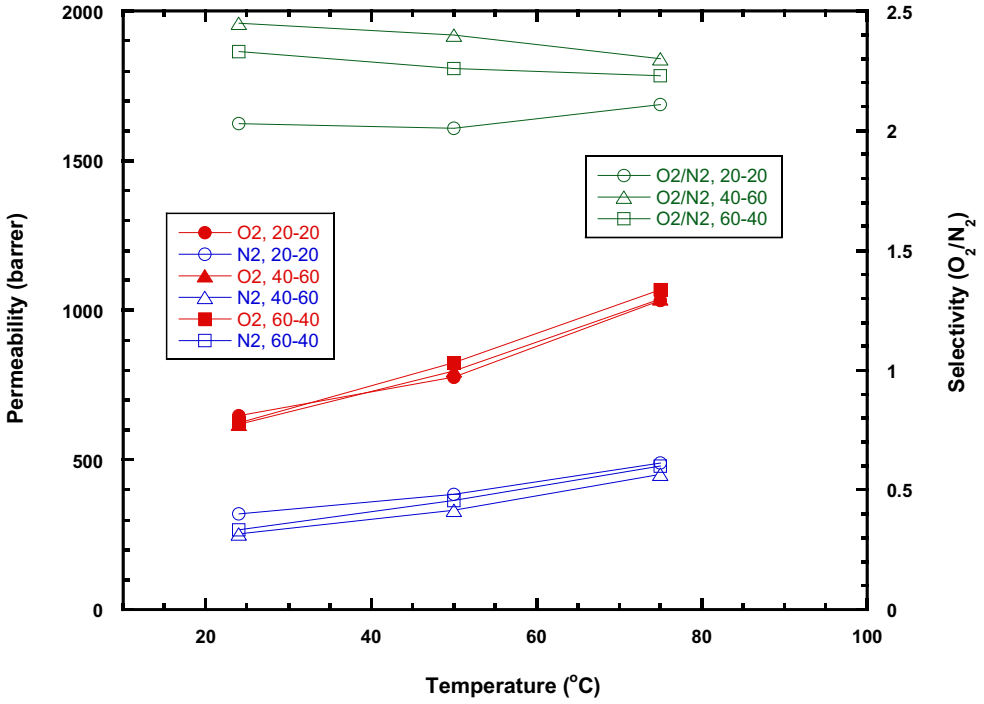

Figure 11. Variable temperature performance of PDMS against O_2/N_2.

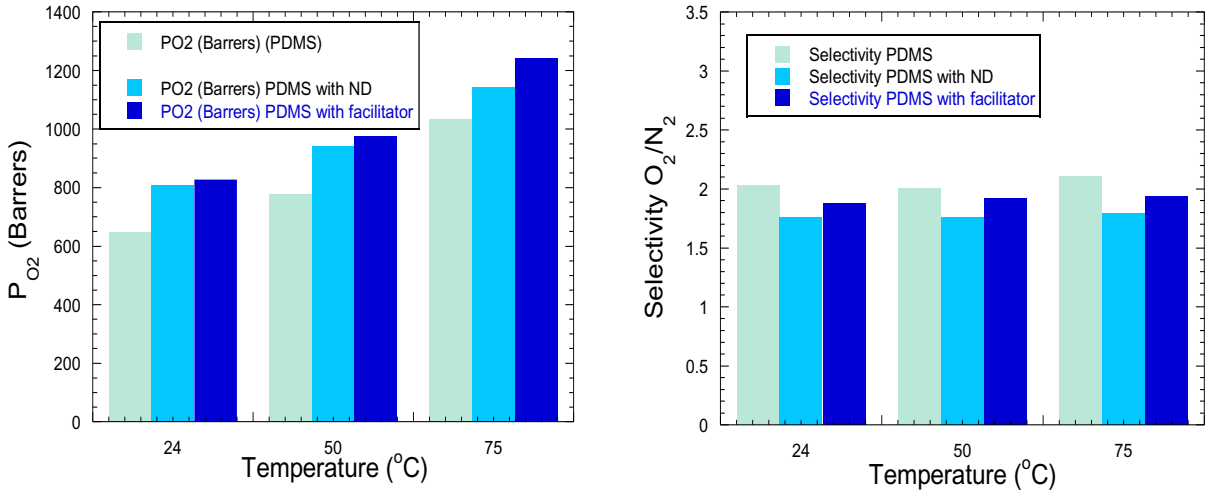

Figure 12. O_2 permeability (left) and O2/N2 selectivity (right) of PDMS membranes neat, and with NDs and a facilitator as a function of temperature.

1.2.3 Task 3. Membrane Characterization.

Thermomechanical Analysis Experiments. To provide further insight into the nature of the association between NDs and their polymer hosts, mechanical measurements were made, which was the focus of the intern project. From prior studies, data suggest PSF-ND MMMs of specific concentrations may pose a significant challenge to the structure and properties of the PSF membrane film. It has been concluded that by incorporating nanodiamonds into the polymer in large quantities, the polymer structure is weakened by agglomerated nanodiamonds. These agglomerations are envisioned to disrupt polymer chain packing and form defects that would decrease the strength of the polymer. Low concentrations of nanodiamonds

are thought to pose little to no added weakness to the polymer structure. In fact, literature data suggests that ND can impart slight strengthening of films.[10]

The behavior and strength of these films were studied by testing and comparing tensile strength and/or ultimate tensile strength vs strain of the polymer via material film and fiber testing.

- Tensile stress is defined as the applied load/cross-sectional area. (Note: Stress is assumed to be engineering stress because the change in width when necking occurs cannot be measured directly)
- Tensile strength is defined as the stress needed to break the material.
- The ultimate tensile strength is the maximum load that a testing material can withstand.

At first, we used the Thermomechanical Analyzer (TMA) film and fiber apparatus to measure tensile strength, however the load compacity was limited to a maximum of 1.2 N, which was not high enough to properly stress the material. Since the standard film size previously used for Young's modulus testing would not break at room temperature under the maximum load of 1.2 N, multiple tests adjusting the temperature, rate of force and width of the samples were attempted. By decreasing the width of the sample, the cross-sectional area of the sample is reduced, resulting in a larger stress on the sample with the same maximum load applied. Yet this did not allow us to acquire a baseline set of results on pristine PSF at room temperature. The samples were also manually prepared and measured so data plots for a set of identical procedures differed vastly because the samples sizes and thicknesses differed slightly within a few microns.

With a reduced width at 25 °C a few samples ruptured but not consistently. In addition, some samples demonstrated extreme elongation with necking which had not been previously observed with stress ranging from 40-62 MPa. Samples tested at 0.2 N/min with similar cross-sectional areas did significantly elongate up to 55 % strain with only one sample breaking. When the rate was decreased to 0.1 N/min on similar samples with the same conditions, only one sample did not break but that sample still endured 61 % strain.

When adjusting temperature, it was hypothesized that at lower temperatures the polymer would most likely observe a clean break, and at higher temperatures the polymer would most likely observe elongation and encounter necking and then break. At low temperatures (5 °C), only one sample ruptured, but samples still experienced 10-60 % strain with up to 62 MPa of stress. At higher temperatures (75 °C), all the samples broke with significantly less stress around 30-40 MPa while the strain only ranged from about 7-25 %.

These results did not yield very precise or accurate dataset for developing a reliable baseline. It was determined that an instrument capable of a greater load compacity was needed for tensile testing as well as a die cutter to mitigate error from varying sample sizes. Until this could be arranged, several samples of 1, 2 and 3 % 100 °C processed samples were tested under the same conditions on the TMA. These samples were then grouped according to similar cross-sectional area for comparison. However, these results gave no strong correlations from which structural information could be derived. To address this issue, another mechanical instrument with greater dynamic range was employed.

Instron Experiments. One of the conclusions made from the TMA experiments was that better data required more consistent sample preparation. To address this need, an ISO 37 Type 4 die cutter was purchased for sample prep. Method testing on the Instron UTS (Universal Testing System) was examined using pristine PSF. It was determined that roll grips could be utilized by inserting a small piece of fine grit sandpaper to grip the polymer without tearing or shearing the sample, Figure 13. This method allowed the sample to remain secure in the grips and for a larger amount of stress to cause failure within the

reduced section of the sample. The Instron applies about 3 to 5 times the amount of maximum force capable with TMA, thus providing considerably more accurate data on true tensile strength at room temperature. Six sample runs were examined per each set of membranes to provide a reliable average for comparison.

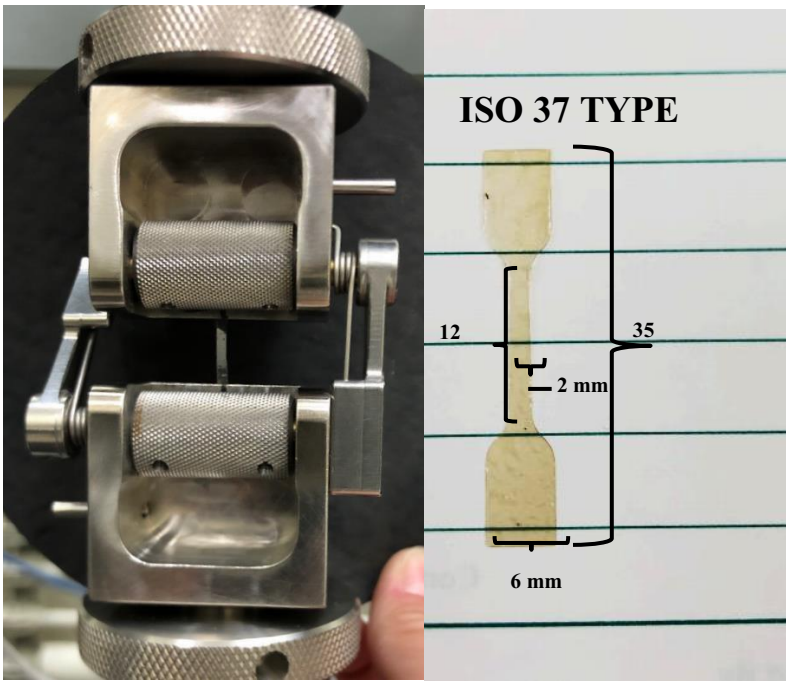

Figure 13. Instron UTS Roll grip fixture and dog bone sample dimensions.

First, it was established that no significant difference was observed between a dated "old" piece of 200 °C processed 2 % PSF-ND and a recently "new" 200 °C processed sheet of 2 % PSF-ND, suggesting the film is highly stable and remains consistent when exposed to air for prolonged periods of time. Second, when examining the average UTS (ultimate tensile strength) of all the samples, the results did not follow the predicted pattern; low concentrations of nanodiamonds within the membrane would pose little to no added weakness to the polymer structure, while higher concentrations were expected to lead to a decrease in polymer tensile strength if NDs formed agglomerates within the polymer structure or higher tensile strengths in the absence of ND agglomeration.

When looking at the data, Figure 14 shows that all the ND containing samples had lower UTS values than the pristine material. Also, the processing temperature did impact slightly the UTS values as well. For the 0 % PSF-ND example, there was a little over a 15 % increase in UTS when the film was only processed at 70 °C compared to 200 °C. The commercial PSF film (UDEL 1700) average UTS was higher than that for cast films processed at 200 °C, but lower than that for 70 °C processed films.

For the ND containing samples, the UTS of the 3 % PSF-ND gives the highest value, followed by 2 % PSF-ND, then 1 % PSF-ND. The result of increasing mechanical strength with increasing ND concentration is consistent with literature reports. [10,12]

In conclusion, the initial loss of UTS on addition of NDs, as compared to pristine PSF, is not well understood, but the observation that UTS increases with increasing ND concentration suggests that agglomeration is not occurring up to 3 % loading and that the NDs may have a chemical affinity for their polymer hosts.

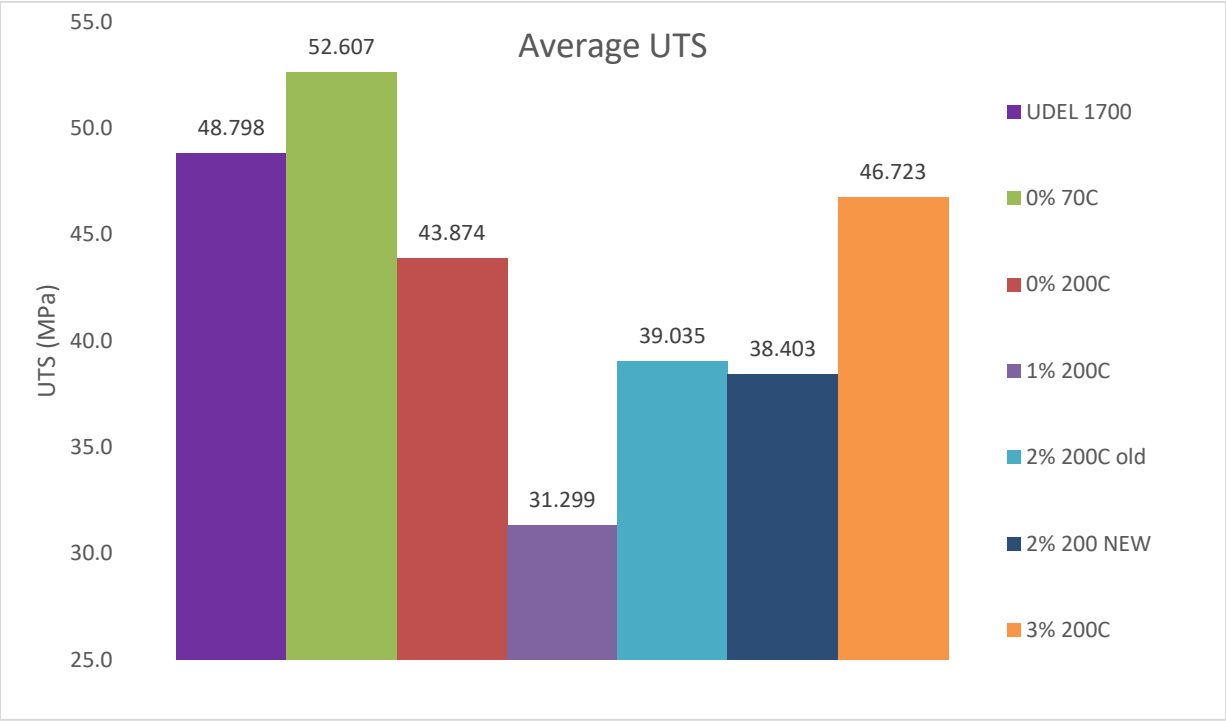

Figure 14. Average UTS collected from the Instron universal testing system.

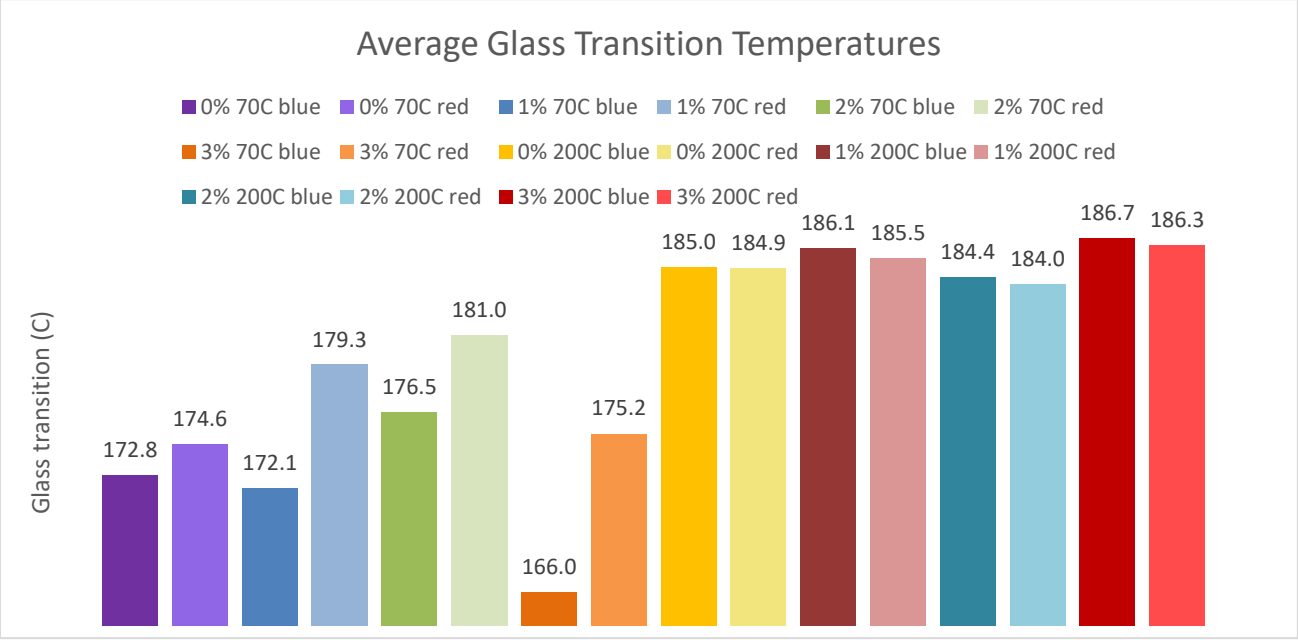

Figure 15. DSC average glass transition temperatures, where the first ramp cycle is 'blue' and the second ramp cycle is 'red'.

DSC Characterization. Differential Scanning Calorimetry (DSC) was utilized to obtain and compare glass transition temperatures (T_gs) between 0, 1, 2, and 3 % PSF-ND as well as between the processing temperatures of 70 °C to 200 °C, Figure 15. The procedure that was used involved cooling the sample to -20 °C, then ramping up the temperature at 10 °C/min to 200 °C followed by cooling at 5 °C/min to -20 °C, followed by one repetition of this cycle.

All the samples that were processed at 70 °C observed an increase in average T_g when comparing the first cycle to the second, which can be an indication of solvent loss. Solvent would be expected to plasticize polymer chains, lowering T_g until the solvent was removed, leading to the increase in T_g of the sample. This conclusion is also supported by the 200 °C processed samples, given that there was very little variation from the first to the second cycle T_g. Since it has been shown that 200 °C processing increased gas permeability, it was concluded that the heat processing at 200 °C does not anneal or densify the polymer structure and is necessary to increase gas permeability by removing solvent that otherwise blocked transport channels.

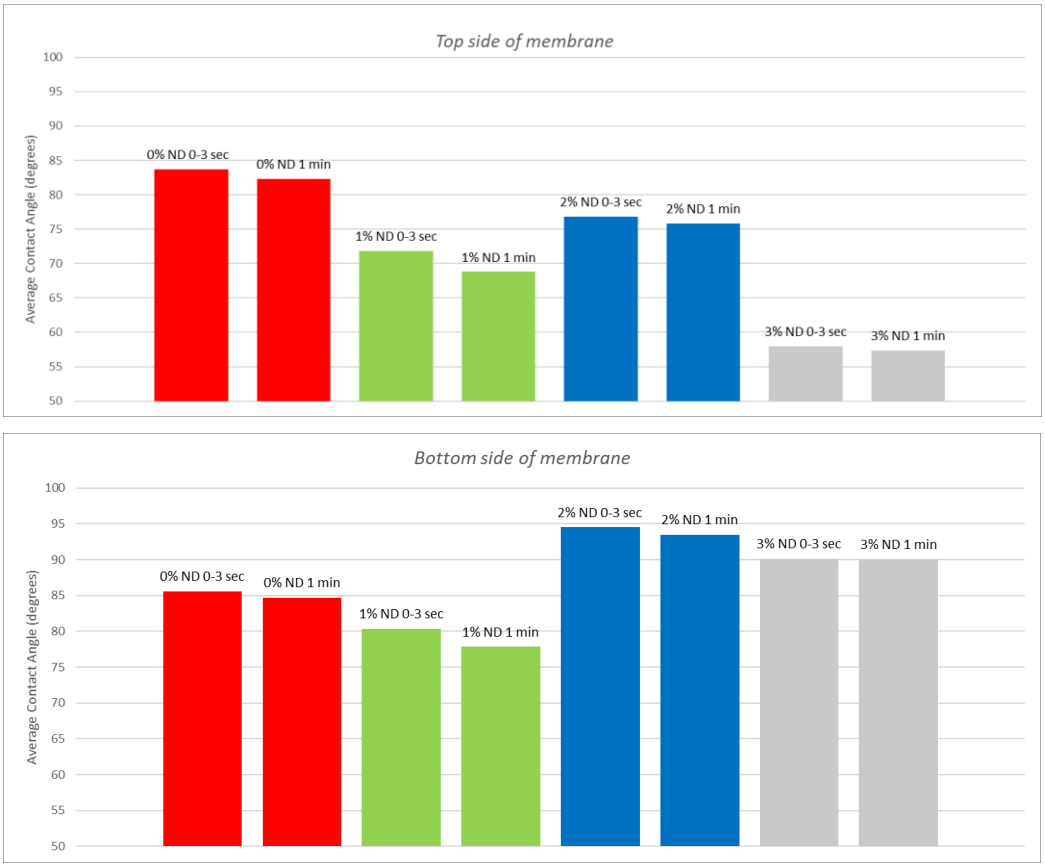

Figure 16. Membrane surface contact angle data for cast PSF (0 % ND), 1 %, 2 %, and 3 % C18-ND. Top surface = upper data, bottom surface = lower data.

Surface Affinity Studies of PSF-ND Composites. Literature reports suggest that NDs make the surface of polymer films more hydrophilic, although this conclusion is not universal. [6, 13-15] The goal of these experiments was to gain insight into the location of NDs in cast films. Questions included: 1) are they evenly distributed; 2) are they unevenly distributed creating an asymmetric structure; and 3) does gravity play a role if asymmetric?

Contact angle goniometry was used to measure the contact angle of a water drop on the membrane surface. The procedure involved measuring the drop over the first three seconds and then making a measurement after one minute, which allows the drop and the surface to equilibrate. Solution cast membranes with 0 %, 1 %, 2 %, and 3 % C18 NDs were used where the top and bottom surfaces, with respect to the casting plate, were analyzed.

Several trends were noted in the data, Figure 16. First, initial (0 - 3 second) drops were slightly larger than those allowed to equilibrate for one minute, which suggests that surface wetting is not an instantaneous process. Second, there is a steady drop in contact angle with increasing ND content, but this did not occur linearly. The 1 % ND data appeared as a standout, where the angles for both sides of the membrane were lower than would be expected from the other three data sets (0 %, 2 %, and 3 % ND loading). However, the fact that the contact angle decreased with increasing ND loading suggests that the NDs are making the membranes more hydrophilic and more easily wet by water. This is considered important because the surface polarity of the polymer can influence morphologies created in phase inversion.

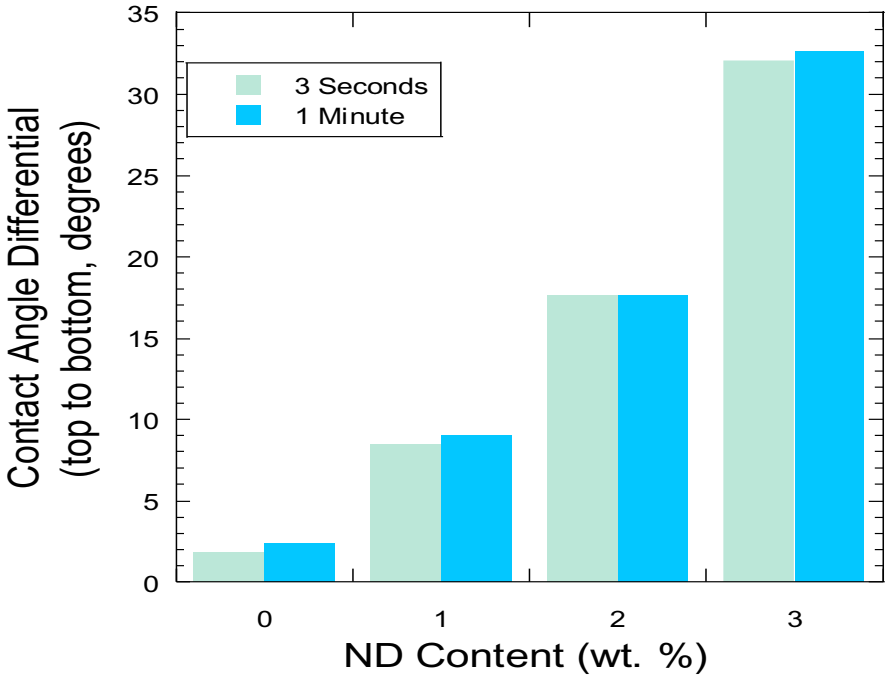

Figure 17. Contact angle differential between top and bottom surfaces as a function of ND loading.

To further understand the results shown in Figure 16, the contact angle difference between the top and bottom sides of the membranes were calculated, and the results are shown in Figure 17 as a function of ND loading. This analysis revealed a trend of increasing difference between the surfaces as ND loading is increased. For pristine PSF, a small difference is noted that is attributed to surface morphology differences between the sides. The top surface of the membranes formed from solution casting have some slight

roughness while the bottom side, formed by contact with the glass plate support, is smoother. From this, it can be concluded that surface effects account for 1-2 ° difference in the data and that differences beyond this amount may be attributed to NDs.

The observation that increasing the ND loading causes increases in the contact angle differences suggests where the NDs may be found within the polymer matrix. That is, the fact that there is a measurable increase in the contact angle difference with increasing ND loading suggests an asymmetric structure where the NDs appear to cluster at the top surface preferentially. This has been reported in the literature before, suggesting that this is not an unreasonable conclusion. [13]

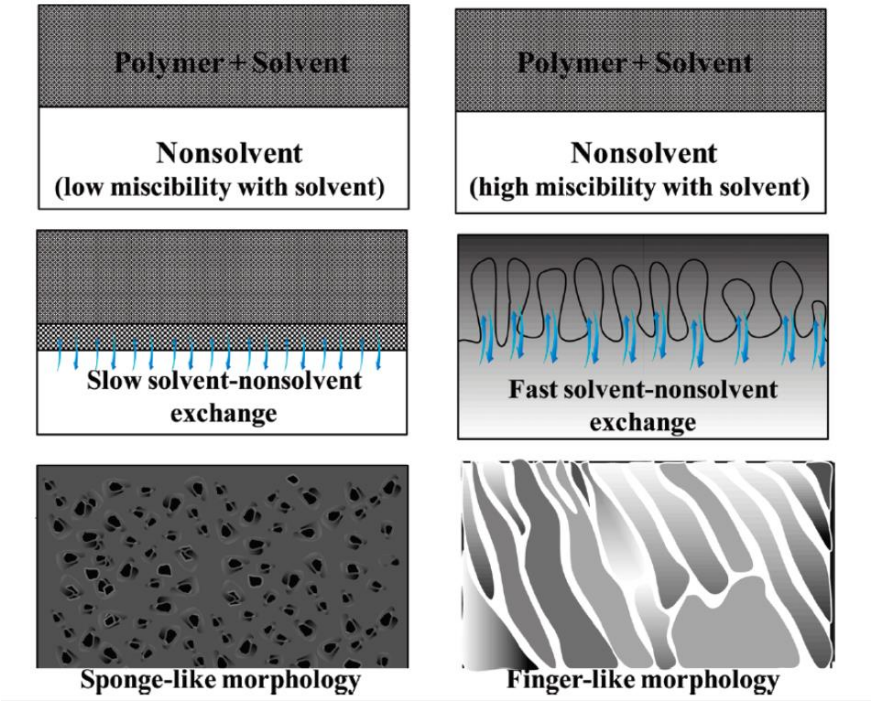

Phase inversion morphology – taken from Hoek et. al, *Ind. Eng. Chem. Res*, 2011, 50, 3798

Figure 18. Morphology pathways for phase inversion.

1.2.4 Task 4. HF Fabrication Development. This task addresses the phase inversion process for PSF-ND materials. Also discussed is the work performed to create multi-layer functional membranes.

Phase Inversion of PSF. Phase inversion is a technique for inducing morphology in polymer materials through a balance of solvent and non-solvent behaviors. Porosity can be created in many polymer materials through exposing polymer solutions to solvents for which the polymer solvent is miscible, but the polymer is not. As Figure 18 shows, the mutual miscibility, and the rate at which the solvent exchange takes place influences the morphology of the polymer product. Slow solvent removal from the polymer results in void formation while rapid removal yields pore structures. *It is important to maintain the ability for PSF to undergo phase inversion to yield porosity, which enables high permeance.*

In commercial practice, phase inversion of hollow fibers is conducted with the polymer dissolved in safe higher boiling point solvent, such as NMP, DMAc, N,N-dimethylformamide (DMF) or dimethylsulfoxide (DMSO). To form the center bore of the fiber, a non-solvent such as water is often used. Likewise, the

non-solvent that causes the formation of the porous structure is also water, which facilitates the removal of the organic solvent from the polymer solution.

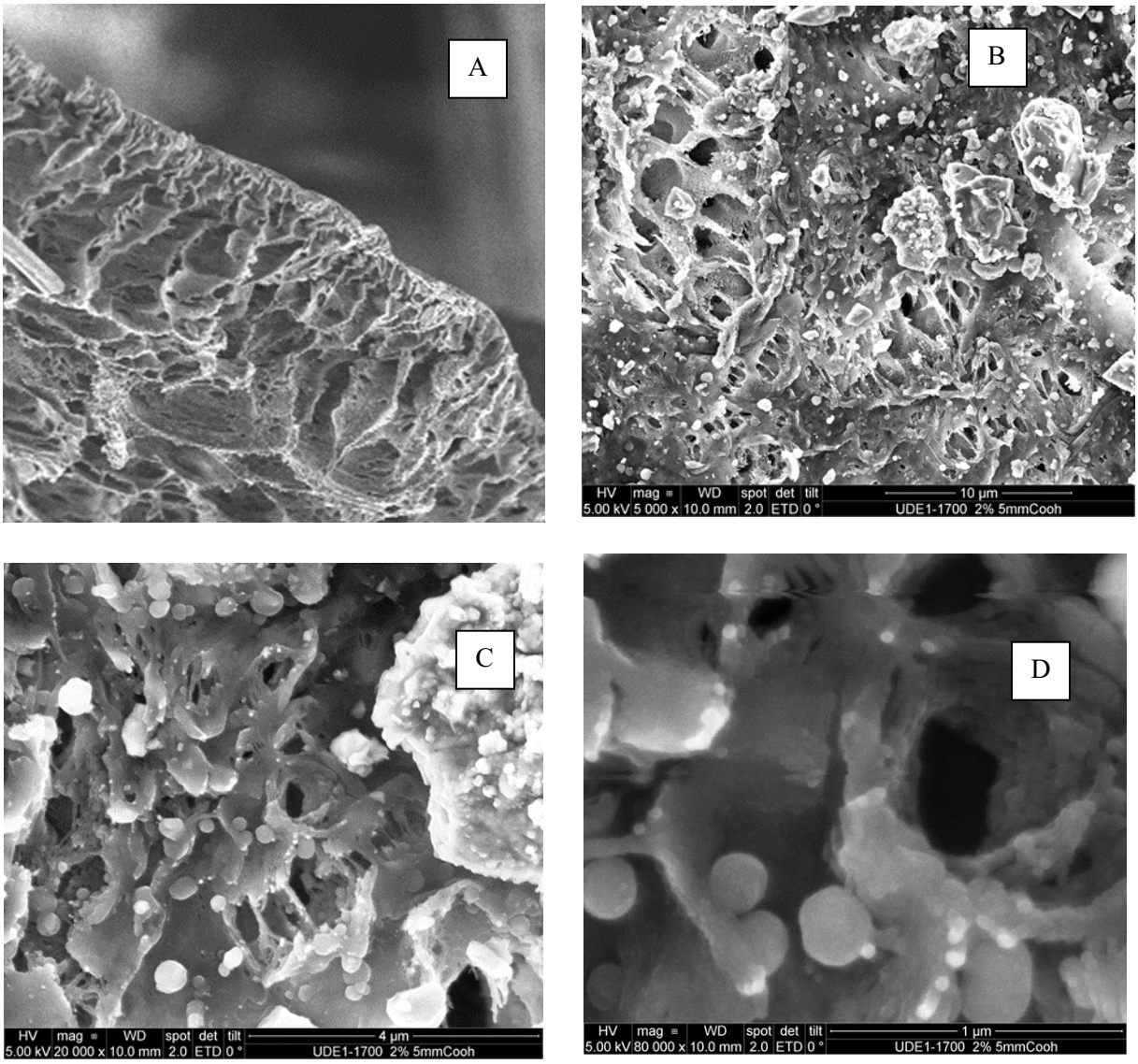

Figure 19. SEM images of phase inverted PSF with 2% COOH-ND.

Given the success of the ND loaded PSF in increasing permeability, it was critical to determine if the inclusion of NDs impacted the ability of the polymer composite to undergo phase inversion to yield porosity. Phase inversion tests on thin films were conducted by first casting the membrane from NMP on to a glass plate and allowing much, but not all the solvent to evaporate. The plate was then immersed into a water bath. Instantly, the polymer film became opaque, which is an indication of porosity. The membrane was then allowed to dry and was available for study. SEM analysis of the resulting morphology are shown in Figure 19, which suggest successful phase separation. Magnification of images follows the order: A < B < C < D. Picture A shows that the cross-section of a film with finger-like pores is evident. Pictures B, C, and D reveal with increasing detail that pores are adorned with ND particles. More clearly,

Picture D shows how the round NDs are attached to polymer surfaces. Another interesting note is that the typical freeze fracture process to yield these images was difficult because the polymer did not tear cleanly, as they do without NDs. This is further evidence of the increase in durability impacted by NDs

A critical question that needed to be addressed to ensure that PSF-ND membranes can be effectively manufactured as hollow fibers is to determine whether solvent retention will be an issue for hollow fiber formation through phase inversion. To answer this question, a phase inverted PSF film containing 2 % COOH-NDs was formed using the aforementioned procedure. After immersion, little effort was taken to remove surface water for fear of removing traces of NMP as well. TGA analysis of this material, Figure 20, shows a large loss of mass below 100 °C, which is attributed to water. Above 100 °C, no significant mass loss is observed until > 400 °C, suggesting that NMP was effectively removed by phase inversion.

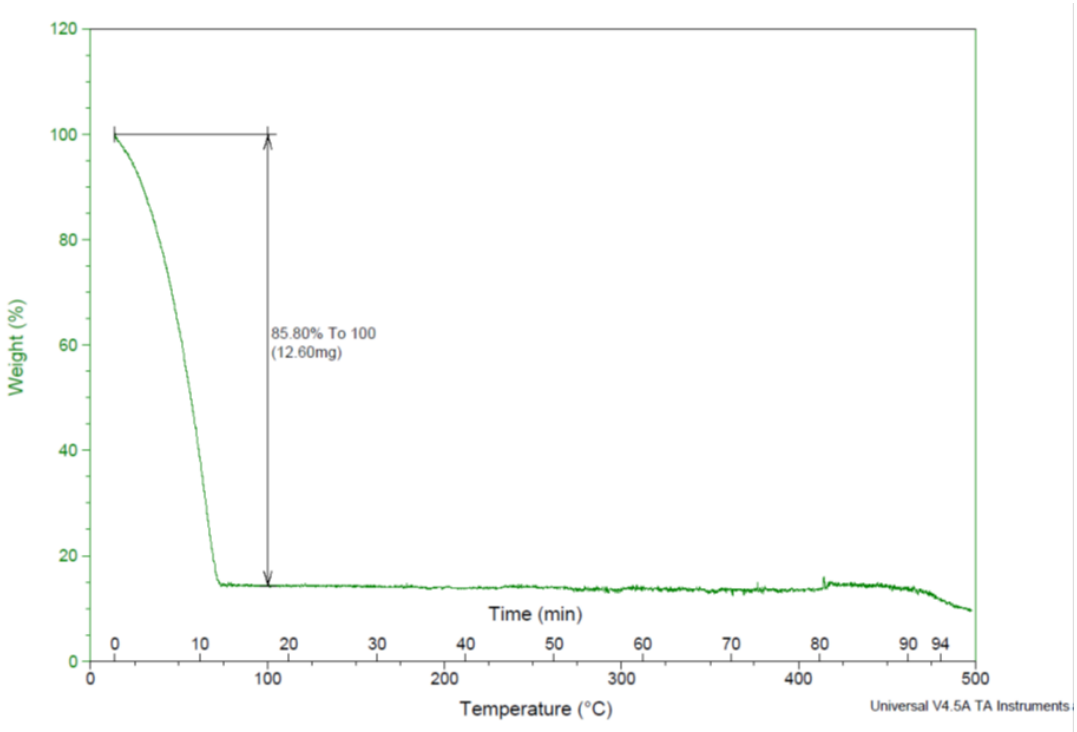

Figure 20. TGA of phase inverted PSF with 2 % COOH-ND.

Table 10. O_2 permeance of phase inverted PSF-ND (2 %) porous membrane supports.

Initial Phase Inverted Membranes (PSF Cast From NMP)	**O_2 Permeance (GPU)**	**O_2/N_2 Selectivity**
No ND's	52054	0.91
2% 5nm-COOH ND (No Heat)	48802	0.91
2% 5nm-COOH ND (Heated to 100 C/10 min)	57007	1.09

Permeance testing of the phase inverted flat sheet PSF-ND (2 %) composites was conducted similarly to that of the dense flat-sheets. Permeance, rather than permeability, is used here because the effective membrane thickness is unknown in porous structures. In this instance, high O_2 permeances were measured, as listed in Table 10. Permeance of 52,000 Gas Permeation Units (GPU) was observed for phase inverted pristine PSF. Addition of NDs at 2 wt. % reduced permeance to 48,000 GPU. However, heat processing of the membrane yielded significantly higher permeance of 57,000 GPU, suggesting that residual solvent, either water or casting solvent, can influence gas flow. Another conclusion was that the NDs qualitatively seemed to encourage better handling behaviors in the membranes that increases the processability of the material and the ease of with which membranes can be fabricated.

Table 11. Permeability data for selected PDMS/phase inverted PSF-ND (2 %) composite membranes.

Membrane	P_{O2} (Barrers)	P_{N2} (Barrers)	O_2/N_2
PDMS cast on 2% PSF-ND phase inverted support (100 µm)	497.0	250.0	2.0
60 µm PDMS placed on 2% PSF-ND phase inverted support (100 µm)	592.3	279.5	2.1
PDMS reference	500.0	250.0	2.0

Multi-layer Membrane Materials. Several multilayer membranes were developed and characterized. First, the gutter layer behavior was probed. In these experiments, PDMS was placed on a phase inverted PSF-ND (2 %) support using two methods: 1) knife casting and curing PDMS directly on to the PSF support, and 2) placement of a 60 µm PDMS film on the support. The permeability results from these composites are shown in Table 11. The data for both PDMS composites closely resemble the reference data for PDMS alone suggesting that the support performs well in that function and that PDMS composite has little to no dense skin layer that would be expected to reduce permeability. Another observation is that the PDMS cast directly on to the PSF-ND support exhibited no visual delamination during the length of the experiment.

Table 12. Permeability data for selected PDMS/PPO composite membranes.

Membrane	P_{O2} (Barrers)	P_{N2} (Barrers)	O_2/N_2
60 µm PDMS placed on cast PPO processed at 150 °C	34.6	12.4	2.8
60 µm PDMS placed on cast PPO with 2% ND content	37.4	8.3	4.5
PDMS layer applied to cast PPO processed at 150 °C	23.1	6.9	3.3

Also investigated was the relationship between the gutter and selective layers. Three differing experiments were conducted. First, a simple composite was formed by the application of the 60 µm PDMS sheet on to PPO cast from toluene and processed at 150 °C. The gas permeability numbers of this composite were similar to that of pristine PPO; however, the selectivity was somewhat lower, Table 12. Replacing the PPO with PPO-ND (2 %) resulted in a slight increase in P_{O2}, a reduction in P_{N2}, and an overall increase in selectivity. In a final iteration, PDMS was knife cast directly on to a cast pristine PPO membrane

that was processed at 150 °C. The permeability data was slightly, but not significantly, lower than was seen for the analogous experiment with the PDMS sheet. Visualization of the impacts as compared to the TEA-informed project goals for two and three stage implementations are shown in Figure 21. The PPO-ND composite yields performance closest to the theoretical upper bound. Taken together, these experiments suggest a good degree of compatibility between the PPO and PDMS membrane materials and predictability of performance.

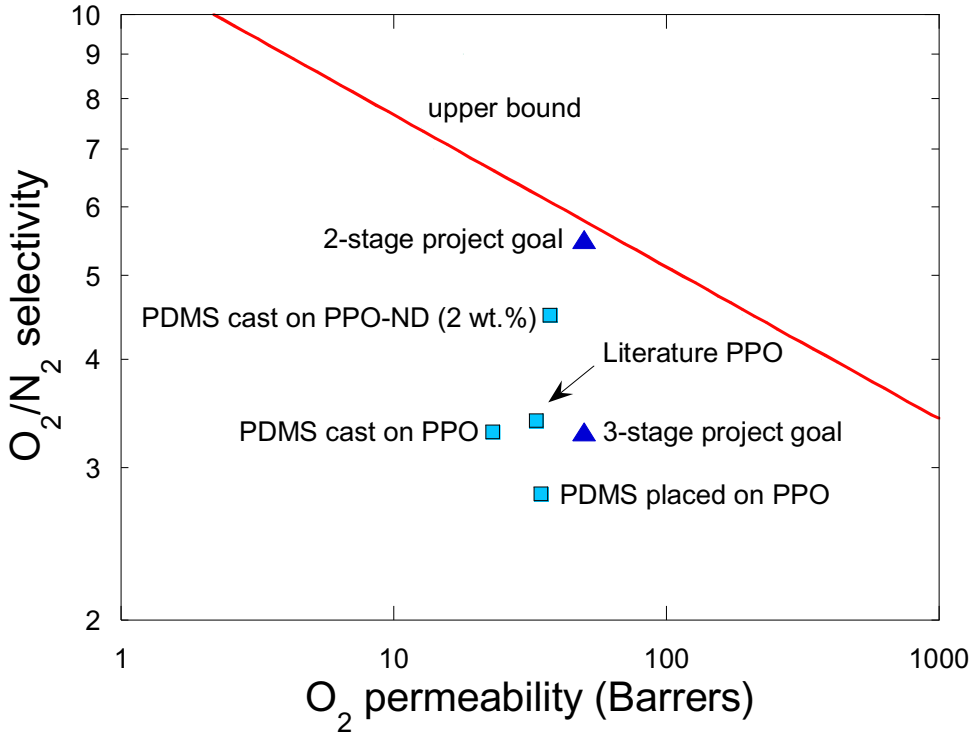

Figure 21. Permeability-selectivity plot for PPO/PDMS layered composite membranes.

An initial attempt was made to develop membrane with all three components: porous support, gutter layer, and selective layer. To form this material, a gutter layer of PDMS was cast on to a phase inverted porous PSF-ND (2 %) composite. A PPO selective layer then was added on top of the gutter layer to form the three-layer composite, Figure 22.

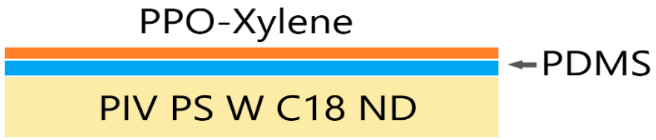

Figure 22. Layer configuration in a prototype multilayer asymmetric mixed matrix membrane.

In the first two rows of Table 13, data are shown for different membranes of the same configuration. There is some variability in the data where selectivity was measured at 5.2 and 6.4. The second line that gave 5.2 is a function of a slightly more permeable membrane to both O_2 and N_2. However, both give acceptable performance in the target application. The performance with respect to the theoretical O_2/N_2 upper bound is shown in Figure 23. Both data points are in the vicinity of the 2-stage performance target

and the upper bound, which suggests that translation of this technology to the hollow fiber format would yield membranes that would meet the economic needs for this application.

The final example used a PPO-ND composite as the selective layer. The data collected for this membrane was substantially lower than the examples that employed pristine PPO. The rationale for this result is not clear, however, NDs may not be suitable additive for PPO selective layers. An important additional observation is that during the study of these new materials, no delamination of the layers was observed.

Table 13. Permeability data for selected PDMS/PPO composite membranes.

Membrane	P_{O2} (Barrers)	P_{N2} (Barrers)	O_2/N_2
PPO cast from xylene and processed at 150 °C, cast PDMS (50 µm), phase inverted PSF-ND (2 %) (100 µm)	29.2	4.6	6.4
PPO cast from xylene and processed at 150 °C, cast PDMS (50 µm), phase inverted PSF-ND (2 %) (100 µm)	32.2	6.2	5.2
PPO-ND (1 %) cast from xylene and processed at 150 °C, cast PDMS (50 µm), phase inverted PSF-ND (2 %) (100 µm)	17.3	4.5	3.8

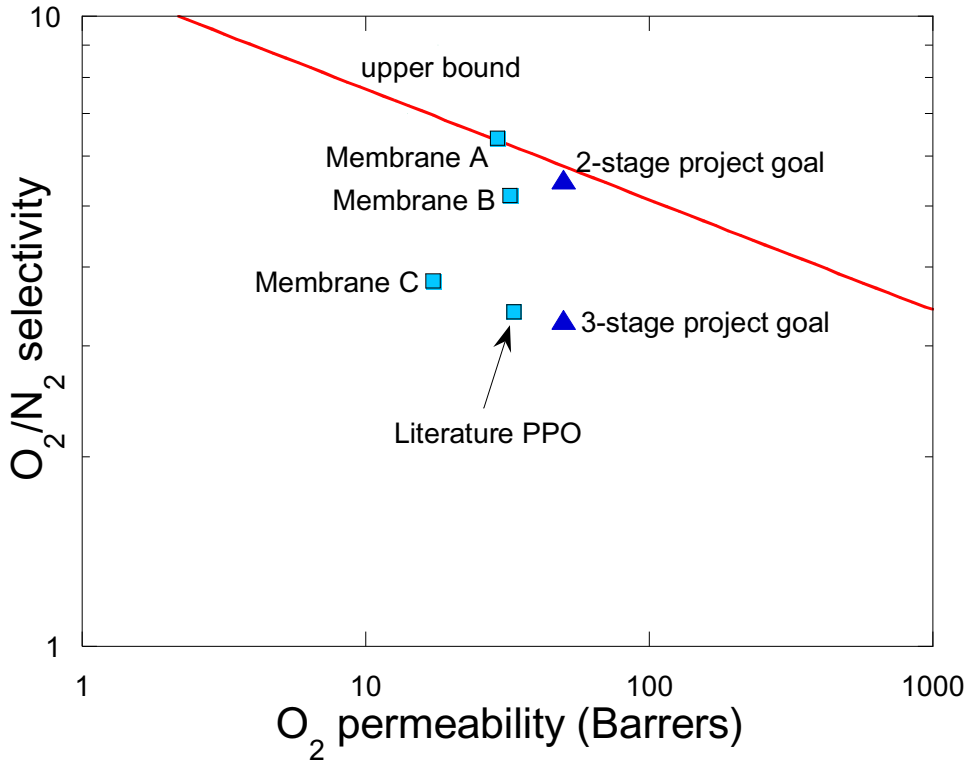

Figure 23. Permeability-selectivity plot for PPO/PDMS/PSF layered composite membranes.

1.2.5 Task 5. Module Development. No work was done on this task during BPs 1 and 2.

Table 14. Model Inputs.

Parameter	Input values
Number of Membrane Modules	1,2 or 3
Material of the membrane module	stainless steel, carbon steel, polypropylene or polyethylene
O_2/N_2 selectivity of the membrane	2-10
O_2 permeance, GPU	100-10000
Inlet volume of air, L/h	100,000 – 16,000,0000
Pressure of inlet air, psi	25-75
Temperature of inlet gas, ˚C	22
Relative Humidity of input air, %	40
Particles in air, ppm	3000
Hours of operation per year	8000
Permeation factor for O_2	0.9
Permeate pressure, psi	14.7
Rejectate pressure, psi	14.7
Permeate temperature, ˚C	22
Rejectate temperature, ˚C	22
Membrane effective thickness, µm	0.1
Temperature of pump, ˚C	22
Material of the pump	stainless steel, carbon steel, polypropylene or polyethylene
Pump efficiency	user chooses
Delivery pressure of a compression pump, psi	25
Vacuum pump pressure, psi	5
Membrane cost, $/m^2	5-50
Membrane installation factor	0.5
Electricity cost, $/kWh	0.04-0.24
Air cost, $/kg	0.0001

1.2.6 Task 6. Modeling/TEA. INL has developed and published a spreadsheet based technoeconomic analysis (TEA) workbook to understand the economics of oxygen-nitrogen separation from air.

1.2.6.1 Technoeconomic (TEA) workbook methodology. An excel based workbook for the TEA was developed based upon the process flow diagram shown in Figure 24. Assumptions, model inputs for the workbook are described in following subsections.

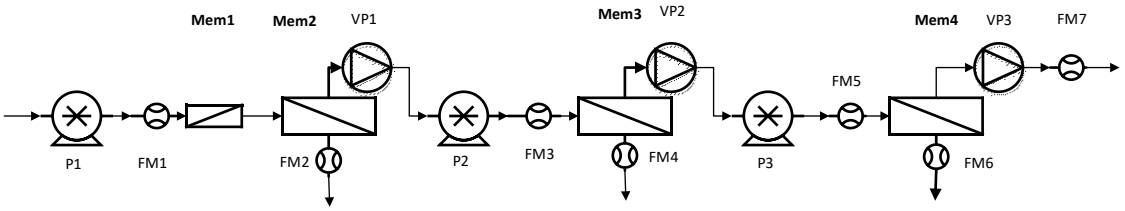

Figure 24. Process flow diagram of gas separation system.

Assumptions. There are some assumptions made in the analysis. If only one membrane is required, although the system is designed with three membrane systems, the last two automatically zero out and only the first one becomes functional. The feed is assumed to be air in all calculations (78.1 % N_2, 20.9 % O_2, 0.9 % Ar, 0.04 % CO_2, 0.002 % Ne, 0.0005 He, 0.0002 CH_4, 0.79 % water). The geometry of the module is also one big assumption: 1 m^2 area of the membrane area is enclosed in one module with volume of 3 L. Also, the gas separation membranes are assumed to be polymeric membranes, the plant life is 30 years, and the capital cost has an interest rate of 6 %.

Model Inputs. For the technoeconomic analysis, several parameters are set as variables in the workbook. Those variables are numbers of membrane modules, material of the membrane module (not the membrane itself), inlet air (pressure, temperature, relative humidity, volume, particles), hours of the operation per year, flux factor of O_2, permeate pressure, rejectate pressure, permeate temperature, rejectate temperature, membrane effective thickness, compression pump properties (material, efficiency, delivery pressure), vacuum pump properties (material, efficiency, vacuum pressure) membrane (cost, system installation, O_2/N_2 permeability, O_2/N_2 selectivity, flux factor, module material). If not otherwise specified, the values tabulated in Table 14 are used for all the calculations. For this study, we have used different commercially available membranes and simulated the results using those membranes.

Mass and Energy Balances. Mass balance is done on every unit of the process flow diagram. The energy balance is performed by assuming the outside atmosphere is ambient air at 22 °C. For the results presented here, the air is itself at 22 °C and energy balance was not necessary.

Capital cost of the membrane system. The membrane system has cost for pumps, membrane material, membrane modules, flow meters, and installation costs associated with the system that includes the data acquisition and control system, land, and other fixed costs. For the material used in the system, the following unit cost of materials are considered as shown in Table 15.

Table 15. Unit price of the materials used in the system.

Material	Unit price ($/kg)
Stainless steel	1.4
Carbon steel	0.3
Polypropylene	0.625
Polyethylene	0.5

Operating, energy and other recurring costs. The system is assumed to operate at Idaho Falls, ID (location of Idaho National Laboratory). The system is also assumed to be run by a full-time equivalent worker, 24 hours a day. Energy cost is associated with the gas compression (pumping system) and vacuum. The plant for each scenario is assumed to last for thirty years and membranes are assumed to last for five years. Annual capital cost interest rate of 6 % is assumed for all the calculations.

Various commercially available and laboratory synthesized membranes are reported to have different O_2/N_2 permeance and selectivity. These data were chosen since they cover the range of performance reported in the literature for polymeric and polymeric-mixed matrix membrane materials, Table 16. [9]

Process Description. The gas separation system comprises a maximum of four membrane units in series. The first membrane unit is a prefilter to remove dirt particles present in feed air. This unit has no gas separation function. A system pump (compressor) is located before this membrane unit. The first gas separation membrane unit follows the prefilter and a vacuum pump is installed on the permeate side of the gas separation membrane to enhance mass transport. This is a technique commonly employed in practice and in TEAs for gas separation systems.

Table 16. Commercially available membranes and their properties.

Membrane	O_2 permeability (Barrer)	O_2/N_2 selectivity
PSU/CNF Mixed Matrix	2.2	3.86
PSU with 20% silica nanoparticles	5	4.5
PPO with SBA 15/CMS/Al_2O_3	10.2	8.3
PSU with 5% microCX	15.3	7.03
PPO, pristine	16.8	4.41
PSU with 5% CX	17.8	5.95
PPO with 20% SBS	18.5	3.8
PI with 6FDA/BATFM	27.1	3.8
PI with 6FDA/PPDA/CF_3	30	4.3
PPO with 1.0% H_4O	32.2	4.6
PI/Glucose TLU at 400 °C	135	4
PI/PVP blend (b) carbon membrane	200	15
PI/Glucose TLU at 425 °C	254	3.8
PI/PVP blend (a) carbon membrane	600	10
PI carbon membrane	812	7.5

The sizing of both the pump, prefilter, the first gas separation unit, and the vacuum unit depends on the feed gas that needs to be processed and gas separation properties (selectivity and permeability) of membrane, as well as the portion of oxygen that needs to be processed at the assigned conditions. The membrane modules following the first module are optional as per the preferred process design. The pumps (both compressor and vacuum) for each membrane unit are also optional after the first membrane

unit. A second gas separation module follows the first unit sequentially where the permeate of first becomes the feed to the second. In the model, a third unit is also considered and operated similarly.

Table 17. Scenario inputs.

Parameter	Input values
Number of Membrane Modules	1,2 or 3
Material of the membrane module housing	stainless steel, carbon steel, polypropylene or polyethylene
O_2/N_2 selectivity of the membrane	2-10
O_2 permeance, GPU	100-10000
Inlet volume of air, L/h	16,000,000
Pressure of inlet air, psi	14.7
Temperature of inlet gas, ˚C	22
Relative Humidity of input air, %	40
Particles in air, ppm	3000
Hours of operation per year	8000
Permeation factor for O_2	0.9
Permeate pressure, psi	14.7
Rejectate pressure, psi	14.7
Permeate temperature, ˚C	22
Rejectate temperature, ˚C	22
Membrane effective thickness, µm	0.1
Temperature of pump, ˚C	22
Material of the pump	stainless steel
Pump efficiency	0.95
Delivery pressure of the gas by the pump, psi	25 each stage
Membrane cost, $/m^2	10
Membrane installation factor	1
Electricity cost, $/kWh	0.12
Air cost, $/kg	0.0001

The sizing of the pumps as well as membrane units depend on the gas volume, the pressure that needs to be generated by the pumps, the vacuum that is necessary and the membrane separation properties, similar first gas separation membrane unit, although it does not need to be the same unit. Ultimately, the system creates a product gas with a certain purity and the model calculates the overall breakeven cost of

production per kg of gas product. The cost of production accounts for the cost of gas product required for a year and it factors in the yearly portion for the costs of capital, labor, energy, and other fixed costs. It also includes raw material costs depending on the materials and membrane that is chosen for the process. The cost of production does not account for the storage and transportation of the product gas.

1.2.6.2 Results. The results here are based on the oxygen required for 5 MWe plant. A 5 MWe plant requires oxygen that is present in 16 million L of 90% O_2 per hour at standard temperature and pressure. The results are presented in $/tonne of O_2 product mixture.

Since a one stage of membrane system (prefilter + one separation module) cannot theoretically give the target product purity of 90% O_2 or better from air, it was important to know how a staged membrane system works in terms of purity and the impacts of additional modules on product gas cost. Our model compares single, double, and three separation stages as a function of cost and purity. The input for these membrane stages is shown in Table 17.

Single stage membrane system. A single stage membrane system consists of a prefilter and a selective membrane unit in a series. For these calculations, two major parameters are varied: 1) membrane permeability and 2) membrane selectivity. For the purposes of the project, these are the data that are being collected in the laboratory on the new PSF-ND MMMs. The system was designed with a pump that delivers pressure at 25 psi. When changing the gas permeance from 20-10000 GPU, the selectivity was fixed at 4, which is a common and practical selectivity. For the calculations where the selectivity range of 2-10 was studied, the permeability was fixed at 100 GPU, which also is practical and readily achievable.

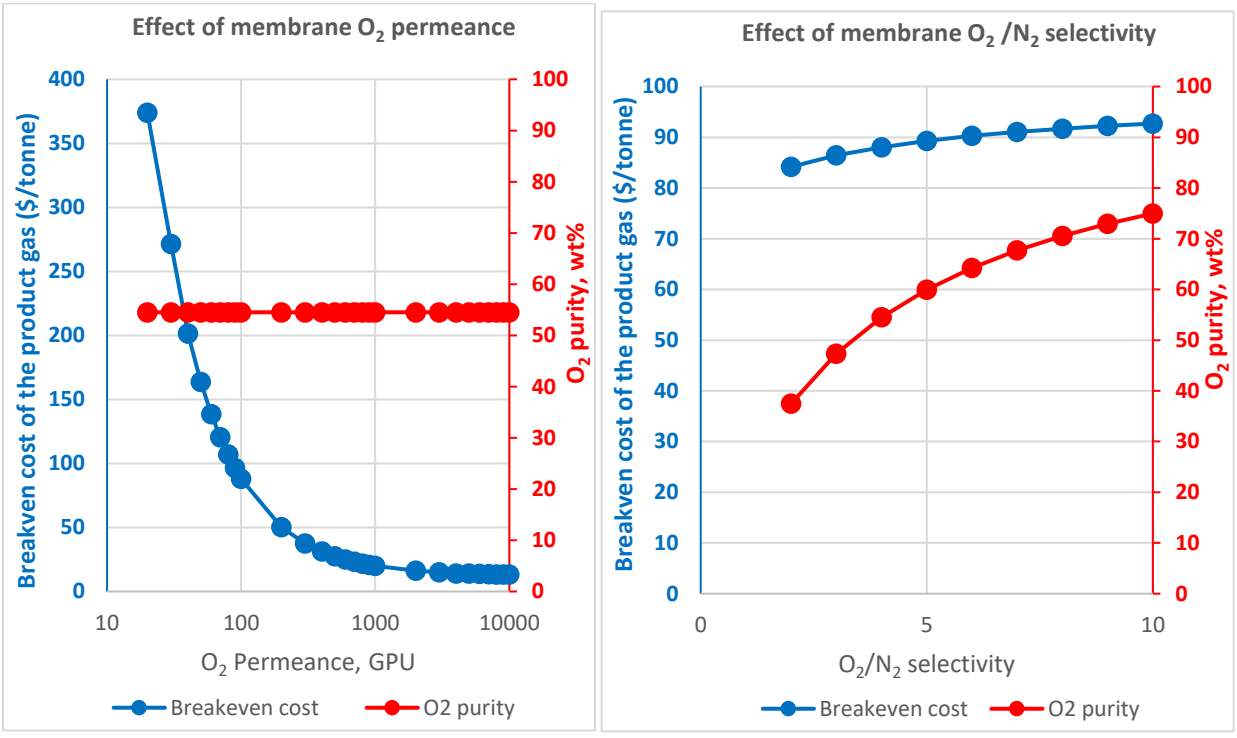

Figure 25. The breakeven cost of product gas production with single stage membrane system.

In the calculation, the cost of production decreases significantly until the O_2 permeance reaches 1000 GPU and after that, the cost levels off at around $20/tonne. This refers to the cost of production of a kg of product gas mixture with 54% O_2 purity. Similarly, by changing the membrane selectivity from 2 to 10 by

keeping the permeance constant at 100 GPU takes the cost of mixture gas from $84/tonne to $93/tonne. At the same time, the purity of the product gas improves from 37% to 75%. The rise in cost per kg of the product gas is explained by the improvement in purity and decrease in overall product quantity. Figure 25 summarizes the results of single stage membrane system.

Different membranes (commercial and literature reported, listed in Table 16) are also analyzed for cost under the same conditions as above, Figure 26. As expected, low permeability and selectivity yielded high cost of gas production. PSU/CNF mixed matrix membrane with the selectivity of 3.86 and permeability of 2.2 Barrer (permeance of 22 GPU) has the highest cost of production of $356/tonne with low purity of 54%. On the other hand, PI/PVP blend (b) carbon membrane with selectivity of 15 and permeability of 200 Barrer (permeance of 2000 GPU) has a very low cost of production of $18.3/tonne and purity of 82%. Figure 26 summarizes the cost of production and purity of the system with selected membranes.

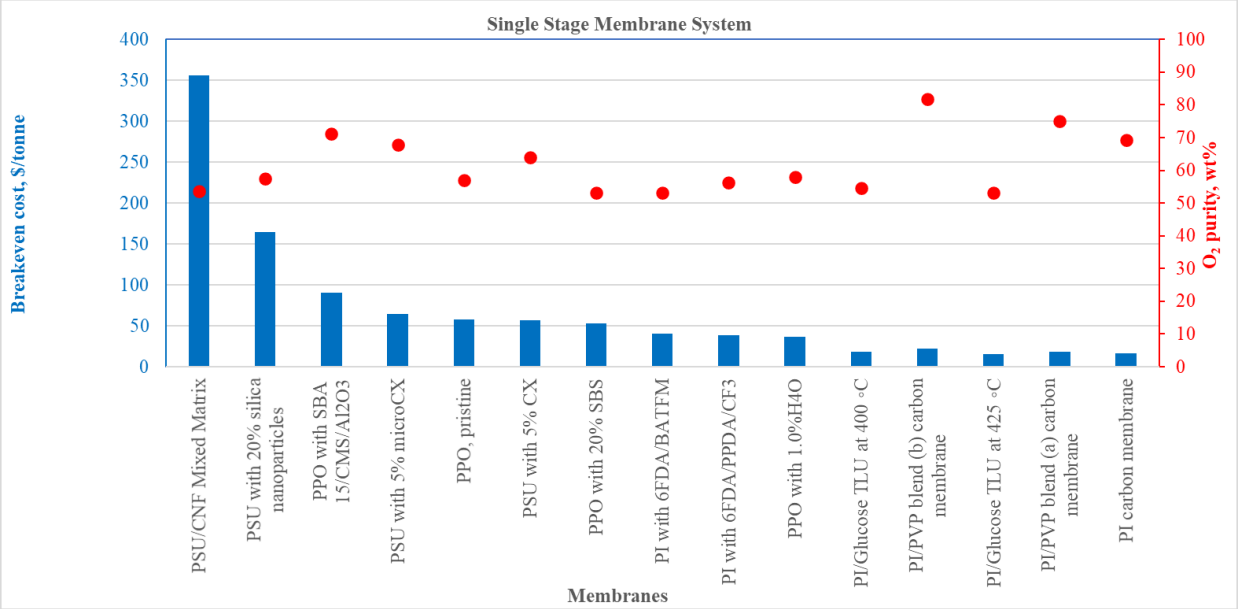

Figure 26. The breakeven cost of product gas production with one staged membrane system for 5MWe plant for various commercial membranes.

Double stage membrane system. A double stage membrane system consists of a filter and two selective membrane units in a series. The permeate gas mixture of first membrane module becomes the feed for the second. For the cost calculations, as was done with the single stage design, permeability and selectivity were varied. The system was designed with a pump that delivers 25 psi to each module. In these calculations permeance was varied from 20-10000 GPU while the selectivity was fixed at 4. Experiments were also performed at a selectivity range of 2-10 while the permeance was set at 100 GPU.

The cost of gas goes up by about 200 % for all cases in comparison to single stage membrane system for cases in which the permeability is altered and the selectivity is kept constant. This is due to a decrease in product gas volume and an increase in energy and capital cost from the second separating module. However, in the double stage system, the O_2 concentration is substantially higher at 82 %, as compared to the single stage approach. The cost of production at 1000 GPU permeance is $58/tonne.

By changing the membrane selectivity from 2 to 10 and keeping the permeability constant at 100 GPU takes the single stage cost of mixture gas of $221/tonne, with a purity of 54.5%, to $225/tonne and a purity of 96.8%. The rise in cost per kg of the product gas is explained by the improvement in purity and decrease in overall product gas volume. In comparison to the single stage system, the incremental

increase in capital cost as well as the decrease in the product volume at the same time contributed to the significant hike in the cost of production. The cost of production by altering the selectivity did not increase the cost but only increased the purity. Figure 27 summarizes the results of double stage membrane system. A conclusion from this analysis is that improvement in permeance appears to have a greater impact on the gas cost than does increasing selectivity.

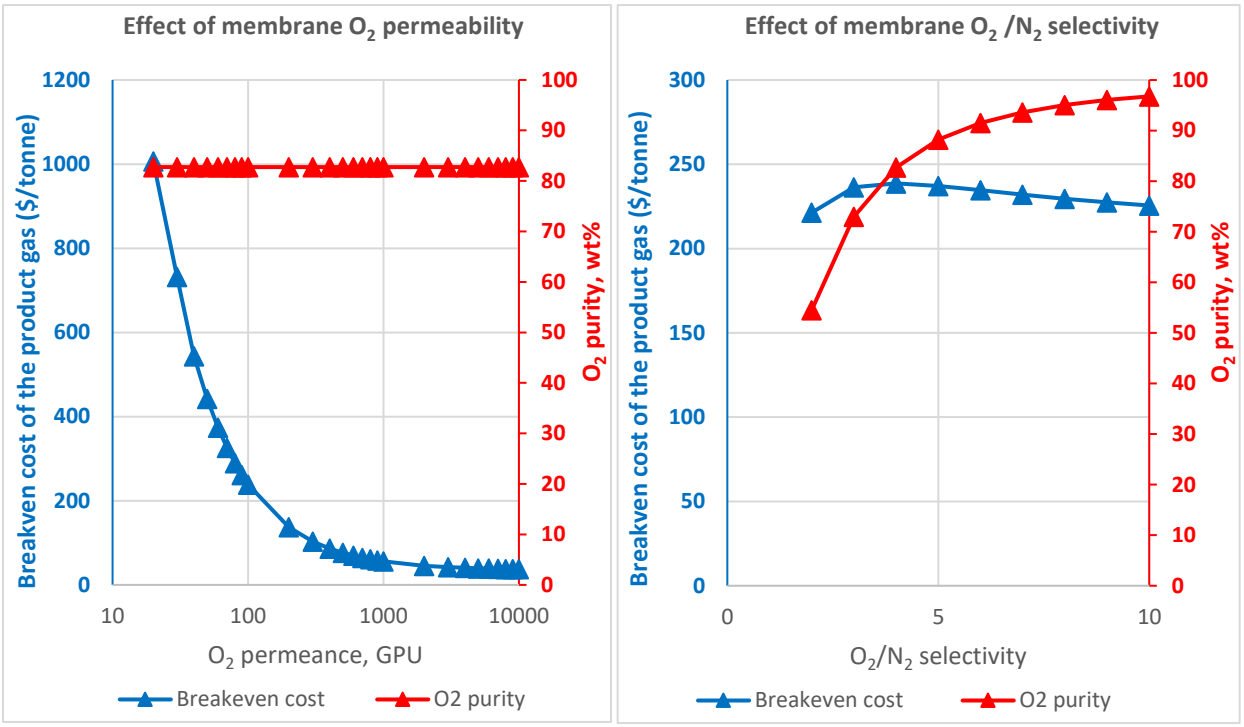

(a) (b)

Figure 27. The breakeven cost of product gas production with double stage membrane system.

Among the commercially available membranes and those reported in the literature, low permeability and selectivity yielded high cost of production in this scenario. Gas production cost also increased significantly in comparison to the single stage membrane system. PSU/CNF mixed matrix membrane with the selectivity of 3.86 and permeability of 2.2 Barrer has the high cost of production of $960/tonne with purity of 81.7%. Conversely, PI/PVP blend (b) carbon membrane with selectivity of 15 and permeability of 200 Barrer has a very low cost of production of $51/tonne and purity of 98.5%. Figure 28 summarizes the cost of production and purity of the gas product for selected membranes.

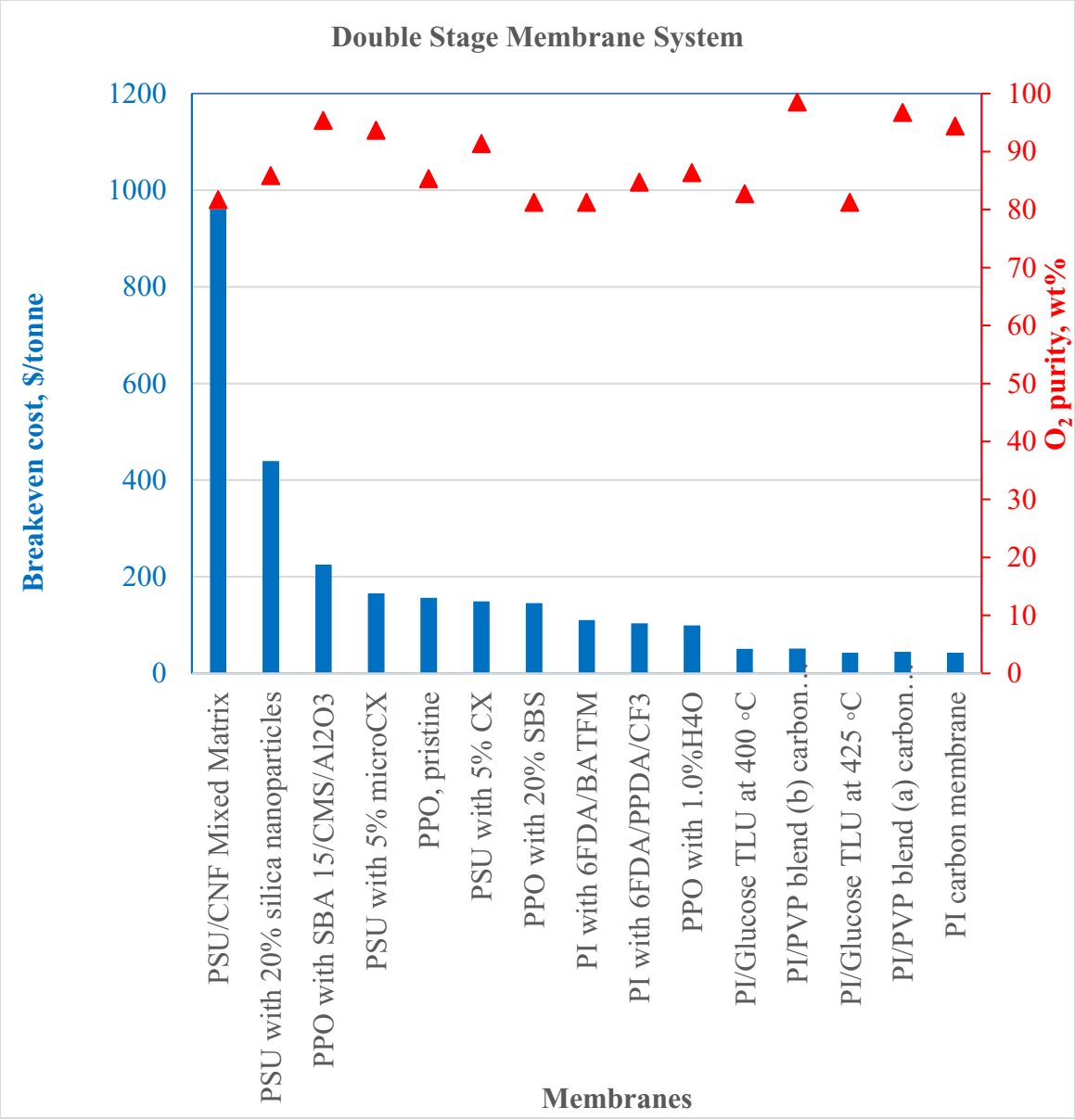

Figure 28. The breakeven cost of product gas production with one staged membrane system at 5 MWe for various commercial membranes.

Triple stage membrane system. A triple stage membrane system consists of a filter and three selective membrane modules in series. Once again, the permeate from each module became the feed for successor units. Analyses were conducted similarly with two sets of experiments: 1) variable permeance at a fixed selectivity; and 2) variable selectivity at a fixed permeance. The selectivity and permeability of all the units are assumed constant, although this is not a requirement. Like the single and double systems, compression and vacuum pumps were used for each unit. Further, experiments paralleled the previous work where 1) the permeance ranged from 20-10000 GPU at a fixed selectivity of 4, and 2) selectivity was varied from 2-10 with the permeance fixed at 100 GPU.

The cost of production of product mixture gases increases by about 65 % for all permeances in comparison to double stage membrane system at constant selectivity. Like the double stage, this is due to the decrease in product gas volume and the increase in energy and capital costs associated with the third module.

However, as more modules are added, smaller modules are used and subsequently, the increment of added cost of production decreases somewhat.

The O_2 purity of the final product is 95 % for the triple stage configuration, which is a significant improvement over the double stage system (82 %). The cost of production at 1000 GPU is $97/tonne which is 67 % more than that of double staged system. Similarly, by changing the membrane selectivity from 2 to 10 and keeping the permeance constant at 1000 GPU, the cost of mixture gas from $408/tonne (purity of 70%) to $225/tonne (purity of 99.7%). The rise in cost per tonne is explained by the improvement in purity and decrease in overall product quantity, in comparison to the double stage system. The incremental increase in capital cost as well as the slight decrease in the product volume at the same time also contributed to the production cost. Cost obtained by increasing the selectivity decreased slightly but increased the purity. Figure 29 summarizes the results of triple stage membrane system.

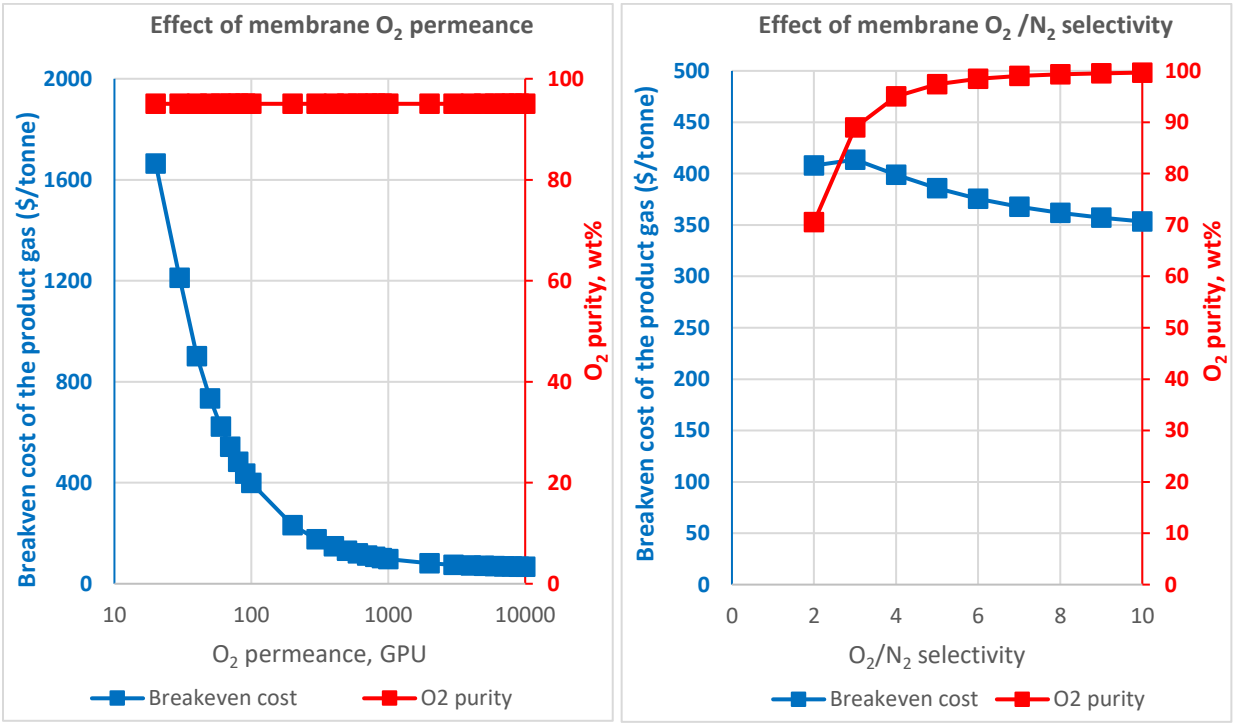

(a) (b)

Figure 29. The breakeven cost of product gas production with triple staged membrane system.

Among the membranes reported in the literature, low permeability and selectivity yielded high cost of production in this scenario as well and this value increased significantly as compared to the single and double stage membrane systems. PSU/CNF mixed matrix membrane with the selectivity of 3.86 and permeability of 2.2 Barrer has the high cost of production of $1597/tonne with purity of 91.5%. However, PI/PVP blend (b) carbon membrane with selectivity of 15 and permeability of 200 Barrer has a relatively low cost of production of $70.5/tonne with a purity of 99.9%. Figure 30 summarizes the cost of production and purity of gas products.

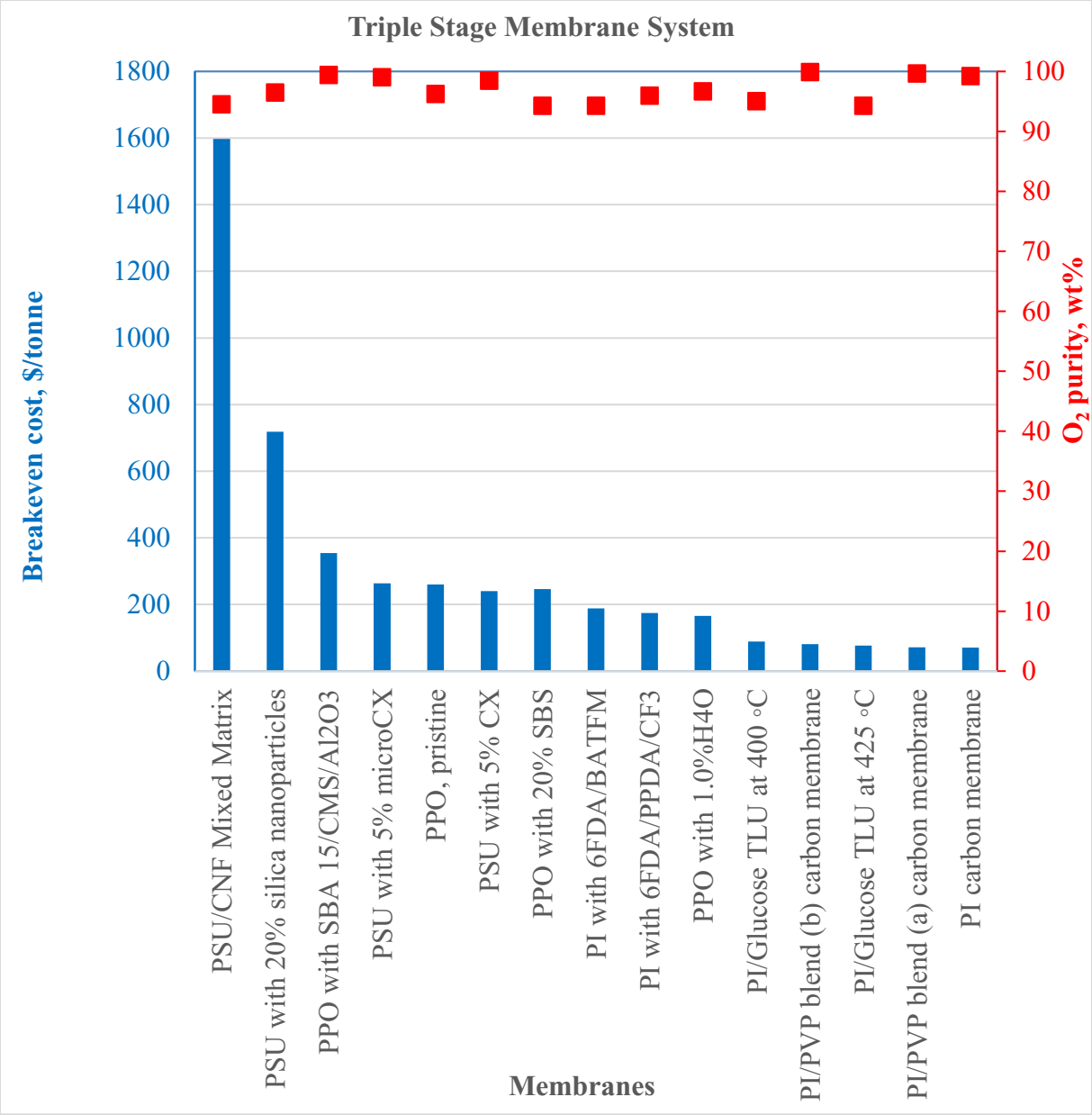

Figure 30. The breakeven cost of product gas production with triple staged membrane system for selected membranes.

Sensitivity analysis. A sensitivity analysis probes individual parameters to assess their importance and contribution to the overall cost of gas production. In this study, specific parameters are selected and varied, which allows for the characterization of their impacts.

Cost of electricity. Providing the driving force, or the pressure differential across the membrane is compression on the feed side and vacuum on the permeate side. This is a common technique to maximize the pressure differential, thus increasing driving force and permeation. The feed side pressure is generated by electrically driven compression pumps and permeate side vacuum is created by rotary vacuum pump. The cost of electricity varies significantly across different parts of the United States. This analysis is meant to elucidate the sensitivity of product gas cost to fluctuation in electricity cost.

The cost of electricity makes biggest impact on triple stage system than in a single or double stage systems due to the additional pumps required for the third stage. If the cost of electricity goes up from $0.04/kWh to $0.24/kWh, the cost of production goes up from $95/tonne to 146/tonne for single stage system, $236/tonne to 323/tonne for double stage system and $377/tonne to $488/tonne for triple stage system. These calculations are based on the membrane with permeance 100 GPU and selectivity of 4. Figure 31 summarizes the results.

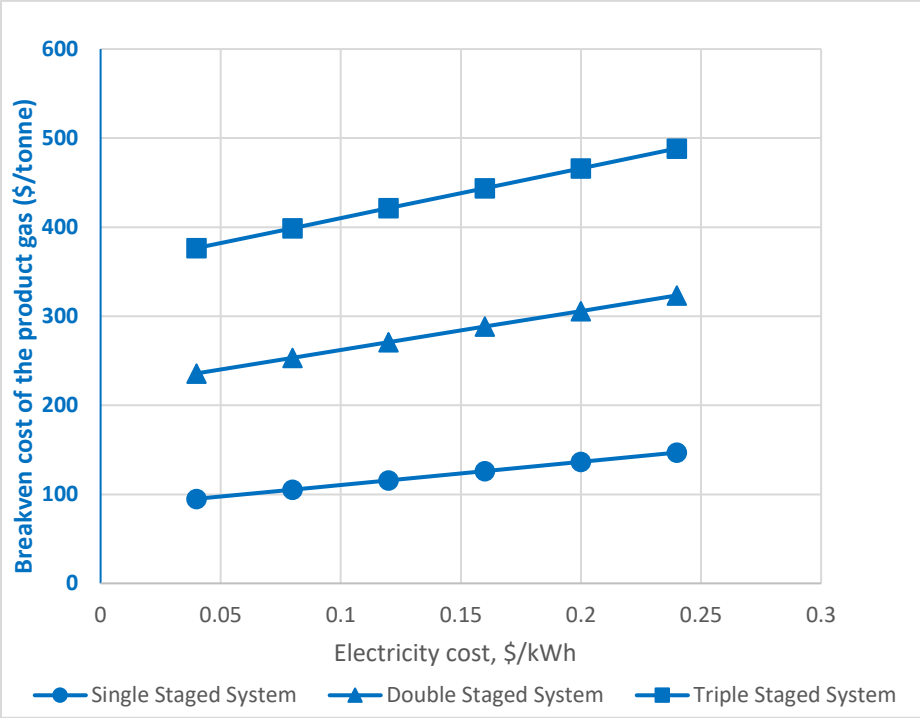

Figure 31. The breakeven cost of product gas production at different electricity costs using a membrane with selectivity 4 and permeability of 100 GPU.

Cost of membrane. The cost of the membrane is a significant contributor to the overall cost of production of product gases. Since the membranes can be selected with different properties and configurations, they have their own costs. For this analysis, the cost of membrane is varied from $1/m^2 to $50/m^2 and cost of productions are calculated.

The cost of production becomes unsustainably high if the membrane cost is $50/m^2 for any of the configurations. Incremental increase in the slopes for cost of production reflects the cost sensitivity due to the larger membrane area. The increment of membrane cost from $1/m^2 to $50/m^2 goes up from $45/tonne to $374/tonne in single staged system, $91/tonne to $975/tonne in double staged system and from $131/tonne to $1589/tonne in triple staged membrane system. Figure 32 summarizes the results.

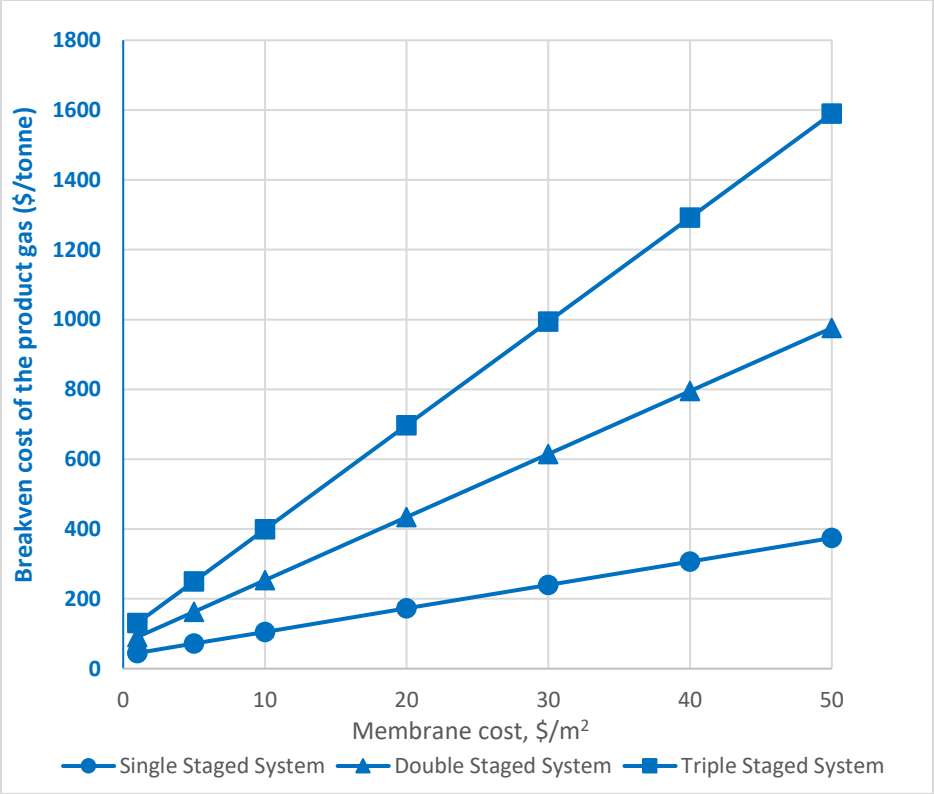

Figure 32. The breakeven cost of product gas production at different membrane costs for 5 MWe plant for a membrane with selectivity 4 and permeance of 100 GPU.

Membrane module materials of construction. When a system requires an increasing number of membranes, module material becomes a more significant contributor to cost. For this study, four different membrane module materials of construction were included: stainless steel, carbon steel, polypropylene, and polyethylene. The cost of these materials ($/kg) is not only different, the Young's modulus of the materials also is different and, as a result, the amount of material and its overall associated cost is different. Stainless steel is the most expensive module material while carbon steel is the least expensive among these four, as summarized in Figure 33.

1.2.6.3 Discussion. Membrane-based gas separation is a promising technology for oxygen enrichment that has various commercial applications. The goal of this analysis is to examine the economics of polymeric membrane oxygen enrichment technology to enable small modular coal generation at a scale of 5 MWe.

Optimized case for O_2 enrichment. Looking at the results for three stage systems and the sensitivity analysis, the best-case scenario for the O_2 enrichment that is closer to and in competition with other existing O_2 enrichment technologies are the ones that are practically achievable with as a high permeability and selectivity as possible to attain 90 % purity. The best-case scenario is achieved with membranes that have a permeance of 1000 GPU and selectivity of 5.5 This yields a cost of production of $58/tonne for a product gas mixture with 90.1% purity using a two-stage approach. Similarly, using three stages, the optimal cost of production for 90.1% O_2 gas is $68/tonne when the membrane is capable of a permeance of 1000 GPU and selectivity of 3.2.

For the best-case scenario two-stage configuration (selectivity of 5.5 and permeance of 1000 GPU), the capital cost investment is $8,191K. The whole production plant is amortized for 30 years and the

membranes are changed every five years. Similarly, stainless steel is used as module material as well as all the associated fittings. Idaho Falls, ID is assumed to be the place of installation.

The membranes incur 10% of the total capital cost in addition to the cost associated with membranes installation (11%) and membrane module material (1%). Compression incurs the remaining cost. The site and other fixed costs are embedded into the system installation portion of the costs.

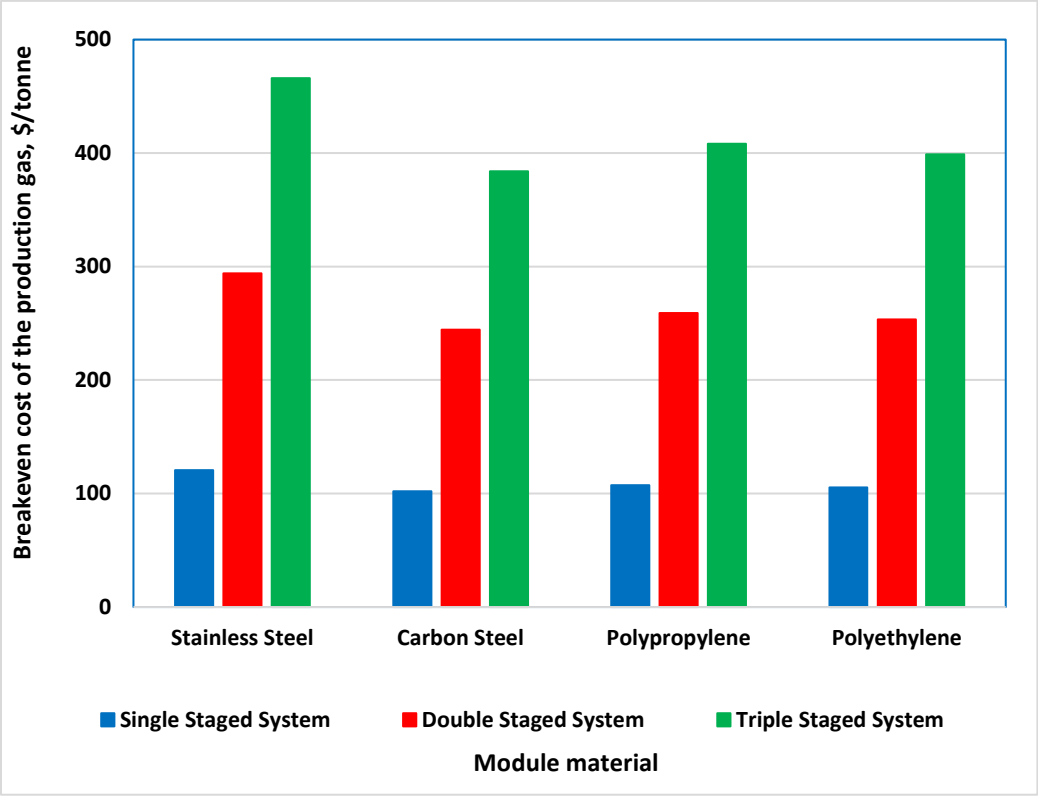

Figure 33. The breakeven cost of product gas production with different membrane module material costs for a membrane with selectivity 4 and permeability of 100 GPU.

By amortizing the capital cost for thirty years, with fixed annual interest of 6 %, capital cost repayment (31 %) incurs for year one a total of $1,927K. Energy cost, with 65 % of total first year cost is the highest followed by operational cost (3 %) of one full time employee. The summary of Year 1 cost break down and capital cost is shown in Figure 34.

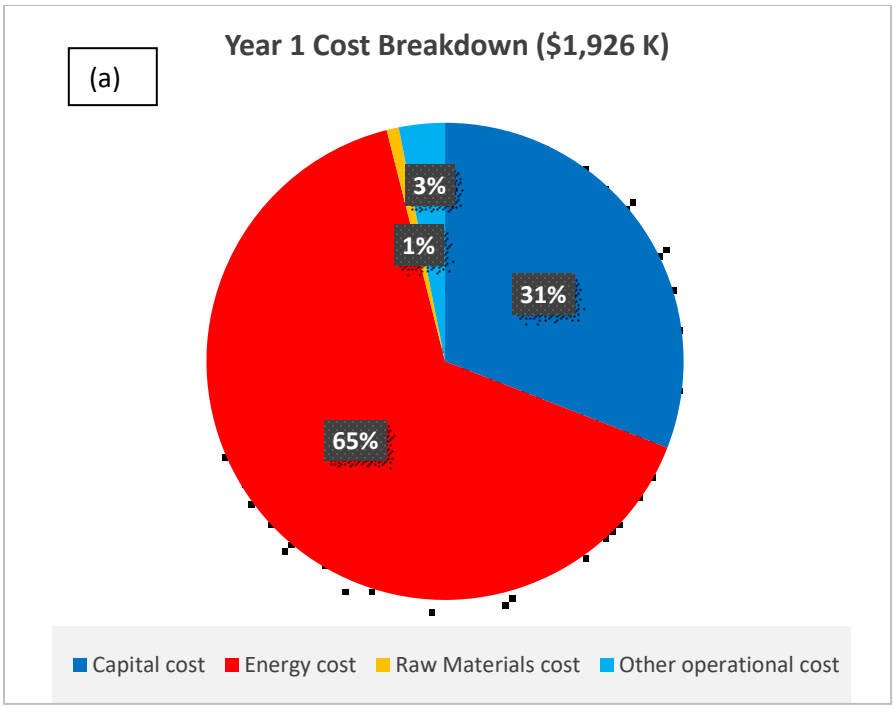

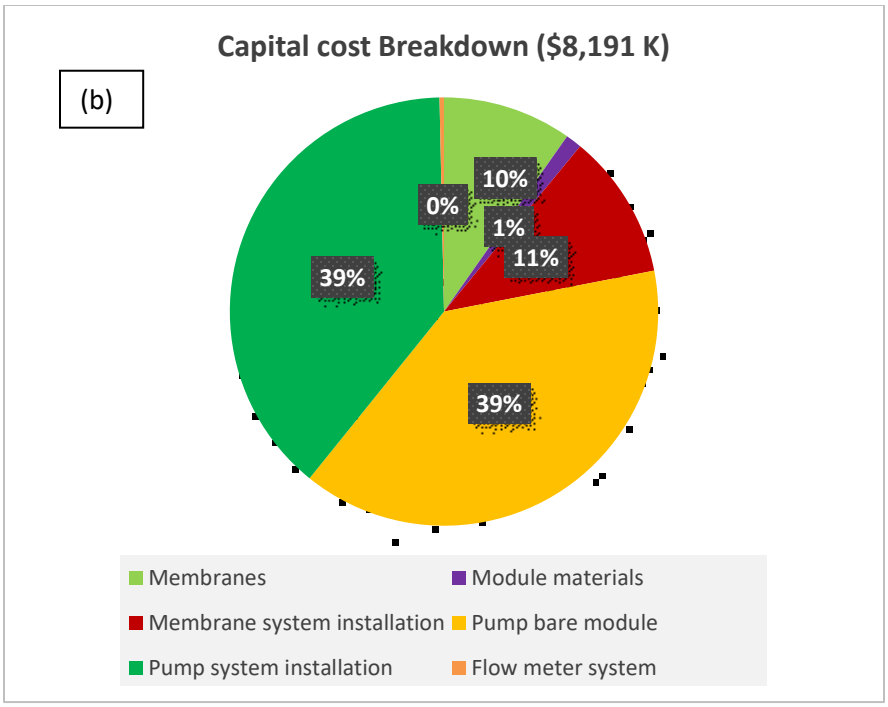

Figure 34. The breakdown of (a) year 1 cost as well as (b) capital cost for the best-case scenario 1.

For the triple stage best-case scenario (selectivity of 3.2 and permeance of 1000 GPU), the capital cost investment is $9,255K and 65 % of the year one cost is due to the energy cost, as shown in Figure 35.

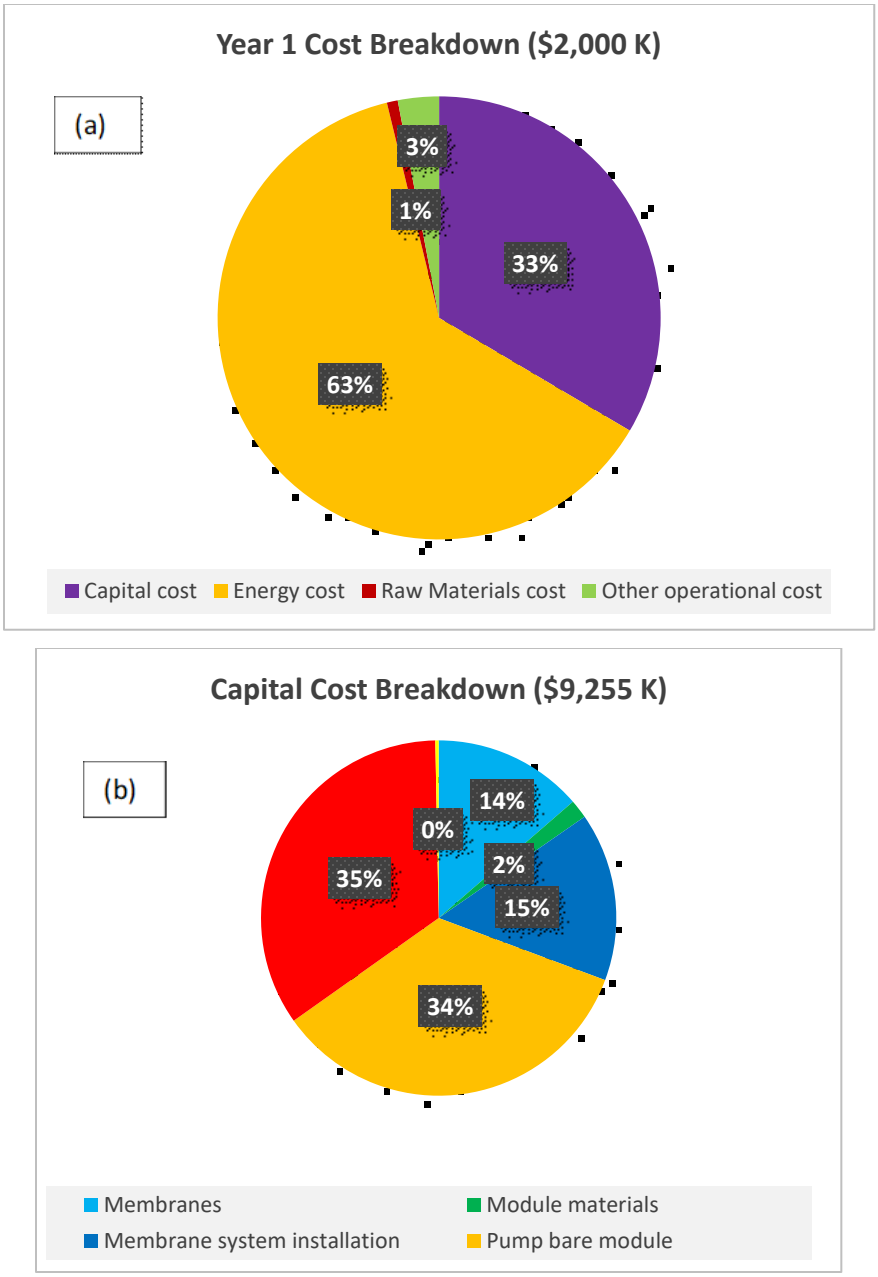

Figure 35. The breakdown of (a) year 1 cost as well as (b) capital cost for the best-case scenario 2.

1.2.6.4 Comparison with other O_2 enrichment technologies

Conventionally, cryogenic distillation and pressure swing adsorption are the dominant technologies for oxygen enrichment. These techniques were considered as a part of this study.

Cryogenic Distillation. Cryogenic air separation technology has been successfully employed for many years to supply oxygen for gasification of a wide range of hydrocarbon feedstocks to generate synthesis gas to produce fuels, chemicals and other valuable products. [16] In fact, cryogenic methods of oxygen enrichment has been in existence for more than a century. Cryogenic distillation consists of at least four major unit operations: air compression and purification, main heat exchanger, cryogenic distillation column, and product compression (internal or external). Air is compressed to 4-10 atm and then cooled to separate the component gases. Oxygen is obtained right at the boiling point of oxygen (90.2 K). Most

of the cost for cryogenic distillation is incurred by the cooling followed by air compression. The major drawback of this technology is it best suited to larger applications due to long start up times, and as a result, the cost becomes high and undesirable for smaller scale systems, such as 5 MWe coal fired plants. The typical cost for this process reported in technical reports and literature is $45/ton ($0.045/kg). [17] The typical purity of the products from this technology is well above 95%.

Pressure swing adsorption. Pressure swing adsorption is a slightly more expensive process than cryogenic distillation. The reported cost for O_2 production for a 90 % pure product gas is ~$65/ton ($0.065/kg). [17] Most of the cost is incurred on the capital expenditure as well as to refill the chambers after the adsorbents are either lost or deactivated over a long period of performance. The energy cost of the production is the most important operating cost.

Improvements of membrane based O_2 enrichment technologies. The cost of the gas production can be reduced by both improving the permeability and selectivity if permeability is not compromised by trying to improve the selectivity and vice-versa. However, there are certain practical limitations for both permeability and selectivity, and one is not mutually exclusive of the other. [18, 19] Similarly, some membranes which have shown higher permeability and selectivity or either one of the two characteristics individually, can be difficult to manufacture at a large scale. Thus, considering the state of art for gas transport technology, this analysis has indicated that an achievable selectivity of 3.3 with a corresponding permeance of 1000 GPU will yield optimum results assuming that the membrane can be readily fabricated. Furthermore, the analysis also indicates that permeance is more important than selectivity. If a choice must be made, it is best to optimize permeance, rather than increasing selectivity.

1.3 Accomplishment Summary. This project generated several significant accomplishments including:

a) A technoeconomic analysis (TEA) of oxygen enrichment using a multi-stage membrane plant was completed. The TEA provided performance goals of 500-1000 GPU with a selectivity of either 5.5 or 3.3 for a double and triple stage systems, respectively.

b) The first polysulfone (PSF)/nanodiamond composites were formed using solution casting techniques. Optimum loading of diamonds was found at 2 wt. %. Loadings above 5 % resulted in agglomeration and defect structure formation. The importance of removal of residual solvent was elucidated. A method to reduce the residual solvent amount to < 1% was developed.

c) DSC supported the conclusion drawn from the permeability experiments that thermal processing of PSF-ND membranes at 200 °C does not anneal or densify the polymer structure and is necessary to remove trace solvent that can block interstitial spaces necessary for gas transport.

d) The thermomechanical Instron data yielded ultimate tensile strengths (UTS) for pristine PSF, both commercially obtained and cast in-house, as well as for the PSF-ND MMMs. The ND composites appear to have an initially lower UTS values as compared to the pristine materials. However, UTS increases as a function of loadings ranging from 1 to 3 wt. %, suggesting that ND strengthen the polymer host, consistent with literature data.

e) Solution casting of NDs into PSF yielded asymmetric distribution of particles within the polymer host.

f) Poly(phenylene oxide) (PPO)/nanodiamond composites were formed and studied as potential selective layers. It was concluded that the performance of the composites was not sufficiently high to warrant their use.

g) Polydimethylsiloxane (PDMS) was used as a gutter layer. Inclusion of nanodiamonds into PDMS was found to increase oxygen permeability approximately 20%. Addition of oxygen transport

facilitators to increase oxygen permeability was not successful, however this was not exhaustively researched.

h) A phase inversion process for forming porous PSF/ND membranes was developed. High permeance membrane supports were formed and found to have oxygen permeance > 57,000 GPU.

i) The first ND-containing multilayer asymmetric mixed matrix membrane has been formed and characterized. This work met the intent of the peer-reviewers' recommendations #3 and #4, discussed in the section 1.4 below. This initial data was promising given the desired outcomes of the project.

    a. The gutter to support layer interface was explored using gas permeability of formed composites

    b. Selective and gutter layer composites were also studied for gas permeability

    c. Composites consisting of all three layers were formed and their gas permeability was measured.

j) The three-layer prototype membrane gave permeability of 29.2-32.2 Barrers, which equates to permeance of 290-320 GPU, which is lower than the TEA informed goal of 500 GPU. O_2/N_2 selectivity ranged from 5.2-6.2, which is consistent with the two-stage implementation of the technology.

k) The successful development of the three-layer flat sheet membrane material is envisioned to be applicable to translation to the hollow fiber format.

l) We supported two summer interns and one post-doctoral associate during this project.

1.4 Response to Peer-Review Comments. A formal peer-review of this project was conducted in October 2020. Resulting from this review were three recommendations that were acted upon.

R3: *Shift the research priority from flat sheet testing and development to hollow fiber membrane development and testing based on the flat sheet data that has already been generated, especially for gutter and selective membrane materials.*

R4: *Produce and test multilayer membranes to examine possible delamination or layer interaction effects on performance and impacts on permeation properties.*

***Team Response*:** It is appropriate to assert that a shift towards multilayered materials also represents a shift towards the hollow fiber format. The activities to address both comments are largely the same. It is not possible to progress directly to multi-layer hollow fibers without first investigating multilayer flat sheets. The reason for this is that while it is relatively simple to develop multilayered hollow fibers, it would have taken an excessive amount of effort to place them into suitable modules, seal them, and obtain reliable permeability data. Given the limited amount of funding and time remaining on this project, it was determined that using the flat-sheet geometry eliminated the impediments to gaining permeability data posed by hollow fiber development. Experiments using prototype multilayer membranes was discussed in section 1.2.4 of this report. The conclusion of this effort was that multilayered membrane materials supported by PSF-ND porous materials did yield improved O_2 permeance and O_2/N_2 selectivity. Furthermore, no delamination of the layers was observed.

R6: *Provide the O2 recovery and energy consumed per mole of O2 produced metrics (e.g., $/ton O2, O2 purity, O2 recovery, energy consumed/mole of O2 produced, stage cut, moles of O2 produced per square meter of membrane area) in a report to DOE.*

***Team Response*:** The requested calculations were performed, and the data is shown in Table 18.

Table 18. Calculated performance parameters as requested by the peer-review.

Parameter	Double staged system	Triple staged system
$/ton O_2	55.66	78.78
O_2 purity (%)	90.1	91
O_2 recovery (%)	89.9	88.1
Energy consumed/mole of O_2, kWh/moles of O_2	0.00676	0.00886
stage cuts	0.333 (1st stage), 0.622 (2nd stage)	0.428 (1st stage), 0.584 (2nd stage), 0.811 (3rd stage)
moles of O_2/m^2 of membrane area/h	0.328	0.177

1.5 Products

What has the project produced?

a. Publications, conference papers, and presentations

i. Journal publications.

Birendra Adhikari, Christopher J. Orme, John R. Klaehn, and Frederick F. Stewart, "Technoeconomic Analysis of Oxygen-Nitrogen Separation for Oxygen Enrichment Using Membranes", *Separation and Purification Technology*, **2021**, 268, 118703.

ii. Books or other non-periodical, one-time publications. None

iii. Other publications, conference papers and presentations:

Frederick F. Stewart, U. Balachandran, Christopher J. Orme, Tae H. Lee, John R. Klaehn, Andrew P. Han, Kaitlyn M. Hillery, "Novel Mixed Matrix Membranes for Separation of Oxygen from Air: Structure and Function of Polysulfone-Nanodiamond Composites", Presented at the 2020 International Pittsburgh Coal Conference, Pittsburgh, PA, September 10, 2020.

b. Website(s) or other Internet site(s): None

c. Technologies or techniques:

d. Inventions, patent applications, and/or licenses:

Stewart, F.F.; Orme, C.J.; Klaehn, J.R.; Shenderova, O.A.; Nunn, N.A.; Torelli, M.D.; McGuire, G.E.; Lee, T.H.; Balachandran, U., "Mixed matrix membranes formed from glassy polymers with improved gas permeability", US Patent Application 17/174,796, Filed February 12, 2021.

e. Other products: None

2.0 Impact. Advantages of the INL/ANL polymer membrane approach include:

- Lower energy consumption – no need to heat the gas stream or use heat/power to condense or desorb O_2, such as is required with cryogenic distillation, pressure swing absorption, or high temperature ion conducting ceramic membranes.
- Engineering to develop and deploy large surface area membrane modules is mature. Currently, membranes are used in many gas clean-up processes such as natural gas sweetening and vapor capture. The engineering knowledge to make commercial scale membranes in a variety of sizes exists and is mature. This project takes advantage of those engineering successes to propose a solution to the problem of economic O_2 enrichment from air.
- Potentially lower capital cost (CAPEX). Durable fouling resistant membranes will result in longer operating times and lower need of replacement. Membranes will be designed to resist pressure and temperature excursions that are expected to occur in variable operation with the result of achieving lower capital cost due to longer lasting modules.
- Modular, ease of deployment. The engineering to scale membrane systems is mature and robust. New membranes will be able to be deployed over a wide range of scales from laboratory to that suitable for a small modular plant.
- Flexible – designed to interface well with variable load demands with short start-up and shutdown times measured in seconds.

This project is specifically targeted to enabling increased efficiency in small modular coal fed gasification plants by providing a source of 90-95% O_2 from air. However, the applications for O_2 enriched air go far beyond this envisioned use. In a recent study, the O_2 separation market was determined to be growing with a predicted Compound Annual Growth Rate (CAGR) of 8.4 % between 2015 and 2025. [20] Furthermore, the predicted market size for 2025 is $1.3 Billion/year.

Table 19 shows the markets that would be available to this INL/ANL technology. The fact that enhanced combustion is only 20 % of the full market potential for this technology suggests that, if successful, this project can have a very significant impact in several growing industries, which translates to tangible American economic impact.

Table 19. Markets for Low Cost O_2 Enrichment.

Market	% of Overall Potential Market
Medical	45
Enhanced Combustion	20
Water Treatment	25
Other	10

INL and ANL are equipped to bring this potential to fruition through their Technology Deployment departments. Both have a long history of working with industry, deploying technology, and technology

transfer. Furthermore, the DOE has several mechanisms by which lab technologies can be developed jointly with industry, including the Strategic Partnership Program (SPP) and Cooperative Research and Development Agreements (CRADAs). ARPA-E and DOE's Technology Commercialization Fund (TCF) are other avenues that strongly favor industry and a partnership with the lab could facilitate further development support.

Education is another impact from this work. To accomplish the work scope, post-docs and interns were employed to study critical challenges. During the project, two interns were hired to answer questions on materials durability and chemical affinity. The interns performed hands-on instrumental analysis using INL's thermal suite (DMA, TGA, DSC) and a contact angle goniometer to gain valuable insight into the mechanical and chemical properties of PSF-ND membranes. One student based his Honors College senior thesis at Penn State University on work from this project. This student has now enrolled in graduate school and will be pursuing research in membrane science. He was inspired by his work on this project. The other student was a chemistry major at Fort Hays State University, Hays, KS. In her two summers at INL, she performed much of the mechanical testing of the new PSF-ND composites discussed in this report.

In summary, much of the work needed to develop this new technology has not been completed but is a part of the scope moving forward. The utility for inexpensive O_2 separation from air extends far beyond the energy sector. Thus, we believe that this technology will have application in a variety of industries, magnifying the value of the work to the American economy. Another area of impact is the staff development and education mission of the project. Over the course of this work, post-doctoral fellows and interns will play a significant part. We are using this project as a vehicle to educate the next generation of technologists in areas as diverse as process engineering and modeling, chemical engineering, polymer chemistry, analytical chemistry, and materials science.

3.0 Project Outcomes. This project investigated a new technology for developing durable membranes for oxygen enrichment from air that are suited to small scale (1-5 MW) installations. Performing oxygen enriched gasification or combustion at smaller scales cannot rely on conventional technology; cryogenic distillation and pressure swing absorption, to give optimized performance. These techniques are mature and are best used to facilitate medium and larger scale applications. Both processes have significant energy and process demands that respond well to the economy of scale and this advantage is lost in smaller operations.

Membrane processes are frequently touted as the solution to small scale oxygen enrichment; however, the technology is burdened by high cost and poorly performing membranes. The objectives of this work were to define the performance that would give an acceptable and competitive gas product cost and then develop membranes to meet the indicated performance goal. In service of these objectives, novel materials were formed and characterized based on ND containing MMMs. What was concluded is that perhaps the greatest value that NDs create is that they facilitate membrane formation and appear to reduce defect formation, which has resulted in the development of useful PSF-ND support materials. Experiments with ND containing selective and gutter layer materials did yield improvement in O_2 permeability, although the performance improvements tended to be incremental.

The data derived from initial multi-layer membranes was encouraging. Maximum performance of a PPO/PDMS/PSF-ND (2%) composite was found to lie on the theoretical upper bound for the O_2/N_2 gas pair, which represents a significant performance increase over any of the components individually. The physical properties of the resulting multi-layer materials appear suitable for conversion to a hollow fiber format. It was found in this project that the PSF-ND material yielded excellent hollow fibers and the coating techniques are expected to be relatively simple. The potting of coated fibers does require effort to yield reproducible permeability data. Project outcomes include three possible avenues to continue the work.

1) Complete development of a prototype novel hollow fiber membrane module. This would consist of coating and potting hollow fibers membranes for O_2 concentration from air.

2) Use the PSF-ND support material to host other selective layers for other applications. An example is a carbon dioxide capture membrane. Some of the most effective selective layer materials are dimensionally unstable polymers that require robust support. The key to developing higher performance membranes for capturing CO_2 at lower concentrations is to reduce defects to as close to zero as possible. The PSF-ND supports may facilitate this.

3) The observation that NDs facilitate membrane formation for challenging materials suggest that they may impart this ability onto other polymers. For example, polybenzimidazole (PBI) polymers offer the promise of high temperature applications, such as separation of gasifier effluent. However, the durability of PBI materials has been challenging. NDs act to add both toughness and flexibility that may benefit PBI membranes.

4.0 References

[1] Kiadehi, A.D.; Rahimpour, A.; Jahanshahi, M.; and Ghoreyshi, A.A. (2015). "Novel carbon nano-fibers (CNF)/polysulfone (PSF) mixed matrix membranes for gas separation", *Journal of Industrial and Engineering Chemistry,* 22, 199-207.

[2] Golzar, K.; Amjad-Iranagh, S.; Amani, M.; and Modarress, H. (2014). "Molecular simulation study of penetrant gas transport properties into the pure and nanosized silica particles filled polysulfone membranes", *Journal of Membrane Science,* 451, 117-134.

[3] Magueijo, V.M.; Anderson, L.G.; Fletcher, A.J.; and Shilton, S.J. (2013). "Polysulfone mixed matrix gas separation hollow fibre membranes filled with polymer and carbon xerogels", *Chemical Engineering Science,* 92, 13-20.

[4] Robeson, L.M. (1999). "Polymer Membranes for Gas Separation", *Current Opinions in Solid State and Materials Science,* 4, 549.

[5] Pulyalina, A.; Polotskaya, G.; Rostovtseva, V.; Pientka, Z. and Toikka, A. (2018). "Improved Hydrogen Separation using Hybrid Membrane Composed of Nanodiamonds and P84 Co-polyimide", *Polymers,* 10, 828-841.

[6] Polotskaya, G.A.; Avagimova, N.V..; Toikka, A.M.; Tsvetkov, N.V.; Lezov, A.A.; Strelina, I.A.; Gofman, I.V.; and Pientka, Z. (2018). "Optical, Mechanical, and Transport Studies of Nanodiamonds/Poly(Phenylene Oxide) Composites", *Polymer Composites,* DOI 10.1002/pc24437.

[7] Avagimova, N.; Pototskaya, G.; Toikka, A.; Pulyalina, A., Moravkova, Z., Trchova, M.; and Pienka, Z. (2018). "Effect of Nanodiamond Additives on the Structure and Gas-Transport Properties of a Poly(phenylene-isophtalamide) Matrix", *Journal of Applied Polymer Science,* 135,46320.

[8] Robeson, L.M. (2008). "The Upper Bound Revisited", *Journal of Membrane Science, 320(1-2), 390-400.*

[9] Chong, K.C., et al., (2016)." Recent Progress of Oxygen/Nitrogen Separation Using Membrane Technology", Journal *of Engineering Science and Technology*, 11(7), 1016-1030.

[10] Kausar, A., (2018). "Nanodiamond Reinforcement in Polyamide and Polyimide Matrices: Fundamentals and Applications", *Journal of Plastic Film and Sheeting*, 34(4), 438-457.

[11] Karami, P., Khasraghi, S.S., Hashemi, M., Rabiei, S., Shojaei, A., (2019). "Polymer/Nanodiamond Composites – A Comprehensive Review from Synthesis and Fabrication to Properties and Applications", *Advances in Colloid and interfaces Science*, 269, 122-151.

[12] Hou, H., Ploini, R., DiVona, M.L., Lui, X., Sgreccia, E., Chailan, J-F., Knauth, P., (2013). "Thermal crosslinked and nanodiamond Reinforced Composite Membrane for PEMFC", *International Journal of Hydrogen Energy*, 38, 3346-3351.

[13] Xu, Z., Zhang, J., Shan, M., Li, Y., Li, B., Niu, J., Zhou, B., Qian, X., (2014). "Organosilane-Functionalized Graphene Oxide for Enhanced Antifouling and Mechanical Properties of Polyvinylidene Fluoride Ultrafiltration Membranes", *Journal of Membrane Science*, 458, 1-13.

[14] Etemadi, H., Yegani, R., Seyfollahi, M., (2017). "The Effect of Amino Functionalized and Polyethylene Glycol Grafted Nanodiamond on Anti-biofouling Properties of Cellulose Acetate Membrane in Membrane Bioreactor Systems", *Separation and Purification Technology*, 177, 350-362.

[15] Bhadra, M., Roy, S., Mitra, S., (2014). "Nanodiamond Immobilized Membranes for Enhanced Desalination via Membrane Distillation", *Desalination*, 341, 115-119.

[16] Smith, A.R. and J. Klosek, (2001). "A review of air separation technologies and their integration with energy conversion processes*", Fuel Processing Technology*, 70(2), 115-134.

[17] Braunberger, B., Richard, A.R., Sethi, V.K., (2019). "Low-cost Oxygen (LCO) for Small-scale Modular Gasification Systems", Thermosolv LLC. https://doi.org/10.2172/1562275

[18] Ye, H.F., et al., (2019). "An adjustable permeation membrane up to the separation for multicomponent gas mixture. Scientific Reports, Article number: 7380.

[19] Freeman, B.D., (1999). "Basis of Permeability/Selectivity Tradeoff Relations in Polymeric Gas Separation Membranes", Macromolecules 32(2), 375-380.

[20] Creedence Research, 2018 (www.credenceresearch.com/press/global-oxygen-enriched-membrane-market